DEDOLOMITIZATION OF JURASSIC TUWAIQ MOUNTAIN FORMATION, RIYADH, SAUDI ARABIA

BY

OMAR ATEF RADWAN

A Thesis Presented to the
DEANSHIP OF GRADUATE STUDIES

KING FAHD UNIVERSITY OF PETROLEUM & MINERALS

DHAHRAN, SAUDI ARABIA

In Partial Fulfillment of the
Requirements for the Degree of

MASTER OF SCIENCE

In

GEOLOGY

DECEMBER 2015

KING FAHD UNIVERSITY OF PETROLEUM & MINERALS

DHAHRAN- 31261, SAUDI ARABIA

DEANSHIP OF GRADUATE STUDIES

This thesis, written by **OMAR ATEF RADWAN** under the direction his thesis advisor and approved by his thesis committee, has been presented and accepted by the Dean of Graduate Studies, in partial fulfillment of the requirements for the degree of **MASTER OF SCIENCE IN GEOLOGY**.

Prof. Michael A. Kaminski
(Advisor)

Dr. Abdulaziz Al-Shaibani
Department Chairman

Dr. Waleed Abdulghani
(Co-Advisor)

Dr. Salam A. Zummo
Dean of Graduate Studies

Prof. Ahmet U. Dogan
(Member)

17/5/16
Date

Prof. Gabor Korvin
(Member)

Dr. Mohamed A. Morsy
(Member)

Dedication

To the Radwans and the Nofals

ACKNOWLEDGMENTS

This study was carried out within the framework of the Research Group on Reservoir Characterization at KFUPM, funded by the Deanship of Scientific Research through Research Group Grant RG-1401.

I would like to express my sincere gratitude to King Fahd University of Petroleum & Minerals and Geosciences Department for giving me this scholarship to study Master of Science in Geology.

I am deeply indebted to my advisor, Prof. Michael Kaminski, and my former advisor, Prof. Ahmet U. Dogan, for knowledge, patience, encouragements, and continually supportive and directive feedback in the process of writing my thesis. Further appreciation goes to Dr. Mohamed A. Morsy for allowing me to utilize the laboratory facilities at Chemistry Department and for the fruitful discussions throughout the research process. I would like also to express my appreciation to Prof. Gabor Korvin, and Dr. Waleed Abdulghani. Many thanks also go to Dr. Dave Cantrell for his valuable comments during the interpretation of the data.

I would specially like to thank Mr. Hatim Dafalla, (Center for Engineering Research – Research Institute, KFUPM) for assistance during analytical work; and Mr. Husam Alzain & Mr. Tarek Akif (Geosciences Department, KFUPM) for assistance in the field.

TABLE OF CONTENTS

LIST OF TABLES

LIST OF FIGURES

LIST OF ABBREVIATIONS

APP: Automated Porosimeter-Permeameter

ICDR: Interface Coupled Dissolution Reprecipitation reactions

ICP-OES: Inductively Coupled Plasma-Optical Emission Spectrometer

mD: millidarcy

PM: Polarized Microscope

SEM-EDS: Scanning Electron Microscope - Energy Dispersive X-Ray Spectrometer

XRD: X-Ray Diffraction

XRF: X-Ray Fluorescence

ABSTRACT

Full Name : Omar Atef Radwan

Thesis Title : Dedolomitization of Jurassic Tuwaiq Mountain Formation, Riyadh, Saudi Arabia

Major Field : Geology

Date of Degree : December, 2015

Two diagenetic processes (chertification and calcitization) distinguish the Jurassic (late Callovian) upper Tuwaiq Mountain Formation (Daddiyah member) in central Saudi Arabia. Field study, petrography, mineralogical analyses, and geochemical analyses were performed on carbonate and chert samples collected from the Khashm Al-Qaddiyah outcrop to determine the distribution, petrography, cause, and timing of the chertification and calcitization diagenetic processes.

While chertification affected the upper third of the Daddiyah member, the dolomite calcitization process affects the whole member and part of the underlying member. Based on studying the texture (fabric-preserving) and relicts (evaporite) within the cherts, the chertification process was found to affect carbonate and evaporite precursors. The dolomite calcitization process displays a series of cementation, replacement, and dissolution fabrics. The source of silica, forming the microcrystalline quartz of the cherts, is biogenic judging from the abundance of sponge spicules in the chert and upper Tuwaiq Mountain carbonates. Vanished evaporite is suggested to be the driving force for the dolomite calcitization process. Their existence is indicated from the carbonate pseudomorphs after lenticular gypsum and evaporite relicts within the cherts. The paragenetic sequence is interpreted in the following sequence: 1) evaporite precipitation, 2) dolomitization, 3) chertification, 4) evaporite dissolution, 5) Dolomite calcitization.

ملخص الرسالة

الاسم الكامل: عمر عاطف رضوان

عنوان الرسالة: دراسة عملية التكلس في متكون جبل طويق، الرياض، المملكة العربية السعودية

التخصص: جيولوجيا

تاريخ الدرجة العلمية: ديسمبر 2015

يتميز الجزء العلوي من متكون جبال طويق ذو العمر الجوراسي، كما ورد في الدراسات السابقة، بعمليتي النشأة اللاحقة؛ التكلّس (تكوّن الكالسيت عقب الدولوميت) وتكوّن الشيرت. وتهدف هذه الدراسة إلى التوصيف الكامل لعملية التكلس؛ توزيعها، سببها، وتوقيتها. في هذه الدراسة تم استخدام الدراسة الحقلية والمجهرية والتحليل المعدني والكيميائي لعينات الصخور الجيرية والشيرت في منطقة غرب الرياض بالمملكة العربية السعودية.

تظهر عملية التكلّس في عدة أشكال؛ نسيج السمنتة، نسيج الابدال، ونسيج الانحلال. وتتركز هذه الأشكال في الجزء العلوي والأوسط من المتكون . ويُعزى حدوث هذه العملية لذوبان المتبخرات (الصخور الملحية) وتفاعلها مع الدولوميت. ويستدل على التواجد المُسبق للمتبخرات في هذا المتكون من بقايا المتبخرات المتبقية داخل صخر الشيرت في الجزء الأعلى من المتكون. وقد فسر ترتيب عمليات النشأة اللاحقة كالتالي؛ ترسب المتبخرات مصاحبا لتكوّن الصخر الجيري، فالدلمتة، ثم تكوّن الشيرت، ثم ذوبان المتبخرات فالتكلس.

CHAPTER 1 INTRODUCTION

1.1 Dedolomitization

Based on experiments and field studies in Styria, Von Morlot (1847) coined the term ‘dedolomite’ to call the secondary calcite occupying the volume formerly taken by dolomite. Later, ‘dedolomite’ and ‘dedolomitization’ were criticized as terms for being ambiguous, geochemically misleading, and inconsistent with the nomenclature for other types of mineral replacements (Smit and Swett, 1969). Instead, others utilize the terms ‘calcitization’ (Smit and Swett, 1969) or ‘dolomite calcitization’ (Scholle and Ulmer-Scholle, 2003) for being a more logical, meaningful, and acceptable name for the replacement process of calcite-after-dolomite. In this study, the three terms are utilized interchangeably.

Most of the early publications related to dolomite calcitization were released in the 1960s and 1970s (Shearman et al., 1961; Evamy, 1963, 1967; Friedman, 1965; Dickson, 1966; De Groot, 1967; Perkins, 1968; Katz, 1968, 1971; Smit & Swett, 1969; Braun & Friedman, 1970; Al-Hashimi & Hemingway, 1973; Hanshaw & Back, 1979; Plummer & Back, 1980). A significant increase in the number of publications in the field was witnessed in the last decade (Figure 1).

Dolomite calcitization is considered to be; a primary hydrogeochemical processes that dominate groundwater quality (Hanshaw & Back, 1979), a tool for authenticating dolomitic marble sculptures (Margolis, 1989), a driving mechanism for karst generation

(Raines & Dewers, 1997), and an analogue process for assessing the long-term behavior of a CO_2 deep geological storage (Prado-Pérez & del Villar, 2011). It is also suspected for the degradation of concrete containing dolomite aggregate (Gillott, 1964). Although porosity changes associated with calcitized dolomite sequences are inconsistent and difficult to predict, they are often characterized by their high porosity which makes them a reservoir for water and hydrocarbons (Purser, 1985). It is also associated with a number of ore forming processes (Boni et al., 2011).

Dolomite calcitization has been recognized as an important process in the diagenetic histories of a wide range of Precambrian (e.g. Kargel et al., 1996) to Phanerozoic (e.g. Bischoff et al., 1994) marine, lacustrine, and terrestrial carbonates. Understanding the genesis of these carbonates is important in reconstructing the geological history of a region. Many field and experimental studies have supported the conclusion that dedolomitization is a surficial phenomenon (e.g. De Groot, 1967; Al-Hashimi & Hemingway, 1973), related to post-burial surface weathering and other near-surface processes associated with subaerial exposure, including the development of unconformities and karstic aquifers. Nevertheless, in some cases dedolomitization can take place during deeper burial diagenesis (e.g. Budai et al., 1984). Calcite does not commonly develop a rhombohedral habit in limestones. Therefore calcite partially or entirely filling rhomb-shaped pore space, or replacing dolomite crystals, constitutes the most straightforward evidence of dolomite calcitization (Figure 2; Coniglio, 1978).

Numerous challenges face the researchers in the field of dolomite calcitization:

A. Several phenomena have been described as dedolomitization and calcitization. ‘Dedolomitization’ term has also been used as an all-encompassing definition to refer

to any alteration affecting dolomite (Fairbridge, 1978). This alteration includes the dissolution of dolomite without precipitating calcite (Acero et al., 2013). It also includes the dissolution of dolomite with precipitating minerals other than calcite; quartz, gypsum, barite, celestite, (Decrée et al., 2008) kaolinite, iron oxides, and smithsonite (Boni et al., 2013). 'calcitization' term is also utilized for other mineral forming process. For instance, calcitization of aragonite grains and cements (e.g. Rabier et al., 2008; Lin et al., 2009; Rogala et al., 2010), calcitization of sulfate minerals (e.g. Stafford et al., 2008; Brasier et al., 2011), and calcitization of silicate minerals (e.g. Hamidi et al., 1998; Giménez-Montsant et al., 1999). About 18% of the studies that uses 'dedolomitization' and 'calcitization' terms are not related to the topic of 'dolomite calcitization'.

B. Dolomite calcitization is a cross-disciplinary field. To fully understand it one has to have a background in thermodynamics, kinetics, geochemistry, and carbonate sedimentology and petrology. It also has applications in many disciplines; petroleum geology, economic geology, hydrology, speleology, archaeology, environmental science, and civil engineering (Figure 3).

C. Although the term 'dedolomite' was introduced by Von Morlot in 1847, 170 years ago, there are still many open questions about the conditions under which calcitization takes place as well as the processes that controls it. The mechanisms and timing involved in the process remain uncertain and are subject of some controversies.

D. There is no comprehensive studies reviewing different aspects of dedolomitization. There have been several important and valuable reviews dealing with this topic (Chilingar, 1956; Friedman & Sanders, 1967; Coniglio, 1978; Flügel, 2004;

Armenteros, 2010; Braithwaite & Heath, 2013). Most of these studies focused on the identification of the dolomite calcitization process (i.e. dedolomite microfahrics) and one of the mechanisms (i.e. reaction of dolomite with calcium sulfate solutions derived from the dissolution of evaporites). Others focused only on one application (e.g. dedolomitization in concrete).

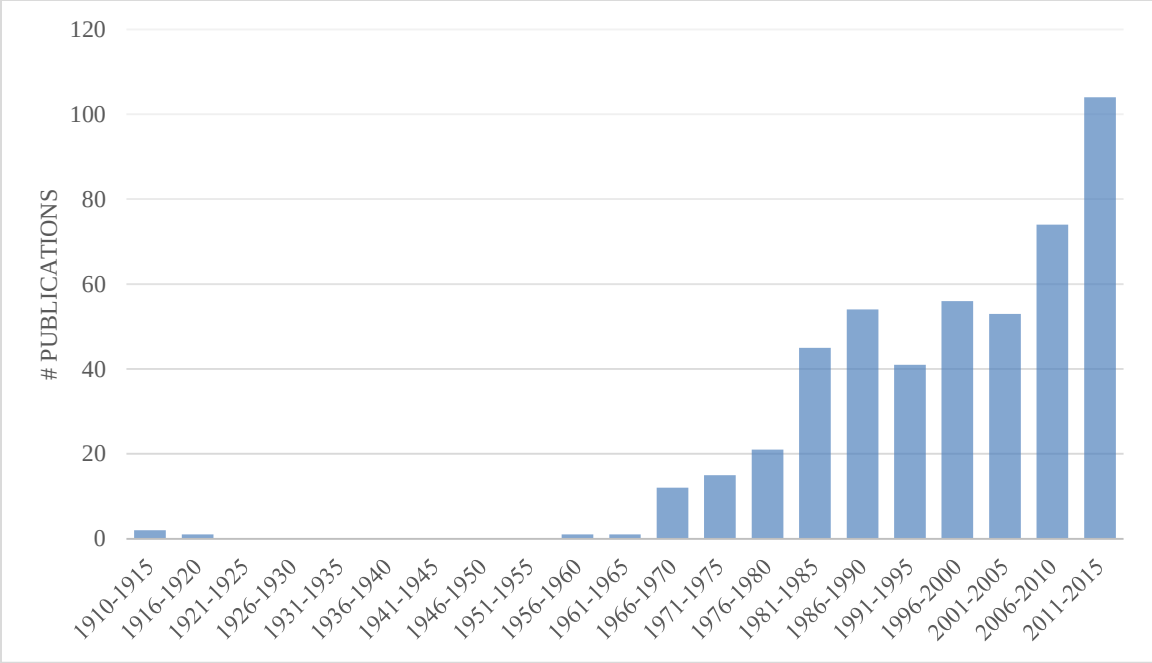

Figure 1. Number of publications in the field of dolomite calcitization increased in the last decade. The data were extracted from the Scopus database using 'dedolomit*', 'calcitization', or 'calcitisation' as key words (accessed 16 Oct 2015).

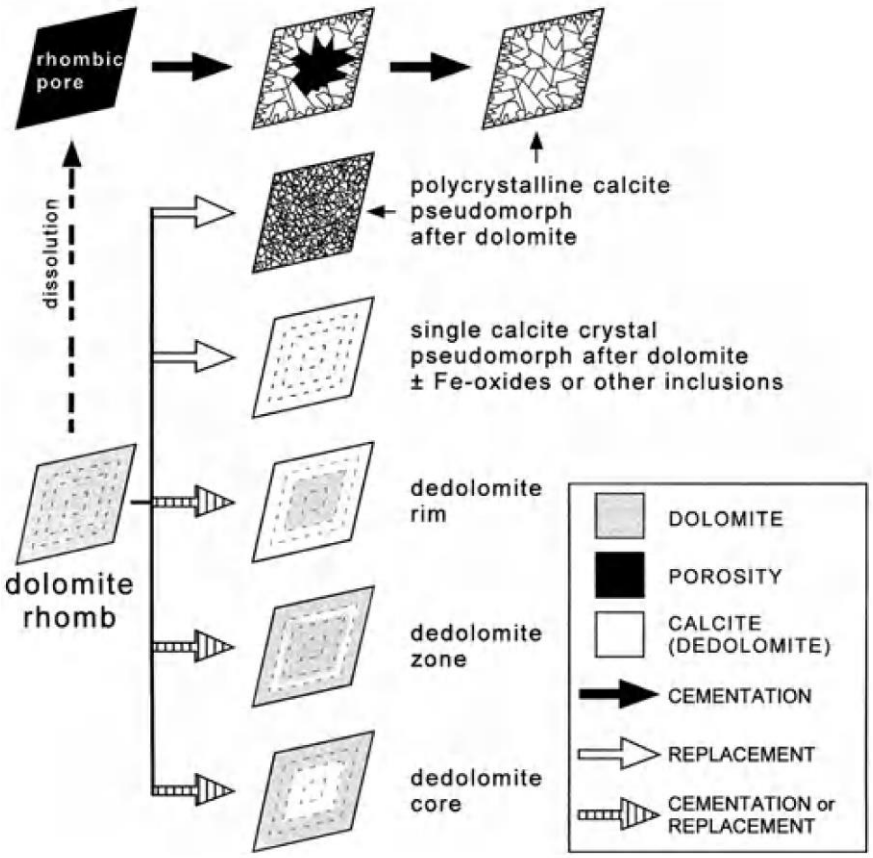

Figure 2. Schematic summary of common dedolomite microfabrics (Coniglio, 1978).

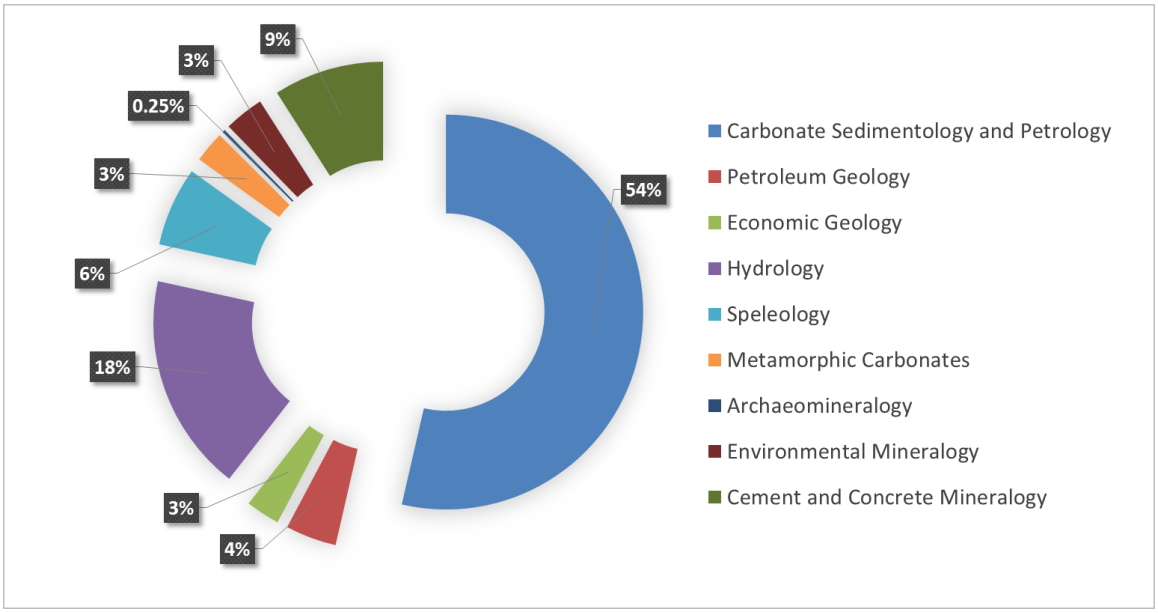

Figure 3. Applications of dolomite calcitization in different disciplines. The data were extracted from the Scopus database using 'dedolomit*', 'calcitization', or 'calcitisation' as key words (accessed 16 Oct 2015).

1.2 Dedolomitization in Saudi Arabia

In Saudi Arabia, dedolomitization was reported in the literature to occur in five formations; Khuff (Khalifa, 2005), Tuwaiq Mountain (Dabbagh, 2006), Jubaila (Cantrell et al., 2007; Basyoni & Khalil, 2013; Eltom et al., 2015), Adgham (Jilh) (Khalifa, 2012), and Usfan (Taj, 2013). Only Jubaila's dedolomitization was studied in detail (Cantrell et al., 2007; Basyoni & Khalil, 2013).

1.3 Tuwaiq Mountain Formation

The Tuwaiq Mountain Formation is a part of the Jurassic Shaqra Group (Mesozoic Dir'iyah supergroup) which includes the Marrat, Dhruma, Tuwaiq Mountain, Hanifa, Jubaila, Arab, and Hith formations (Figure 4: Hughes, 2008). The Tuwaiq Mountain Formation is termed the Sargelu in Kuwait, and the Upper Araej in Qatar and the United Arab Emirates.

The Tuwaiq escarpment represents the major relief feature in central Saudi Arabia. The high-purity limestone of Tuwaiq Mountain enables it to be exploited in many industries; Portland cement, iron metallurgy, paper industry, animal feed stuffs, sewage treatment, and lime manufacture. Parts of the Tuwaiq Mountain are equivalent to subsurface members that host oil reservoirs; Upper Fadhili and Hadriya. Tuwaiq Mountain Formations is considered to be one of the principal source for the oil contained within the southern part of the main producing area of eastern Saudi Arabia.

The Tuwaiq escarpment is the main morphological element in central Saudi Arabia and hence is referred to as the 'backbone of Arabia' (Grainger, 2007). Its height locally

exceeds 200 m and it is found up to 1,000 m above sea level. The escarpment is almost 1,000 km long and extends from the southern margin of the An Nafud in the vicinity of Wadi ArRimah towards the northwestern margin of the Rub'Al Khali, where it is covered by eolian deposits (Figure 5: Rausch et al., 2014). The main escarpment of Tuwaiq Mountain is composed of the cuesta of the Dhruma (mostly obscured by the debris apron) and Tuwaiq Mountain (which forms the vertical cliff face) formations.

During the Middle to Late Jurassic, the Arabian Peninsula was located in the southern margin of the Tethys Ocean, and was the site of an extensive shallow marine platform (Figure 6: Al-Husseini, 1997). The period from the Middle Callovian through the end of the Jurassic represents continued deposition in warm equatorial latitudes. This period corresponds to a sustained global sea-level highstand (Al-Husseini, 1997).

1.4 Literature review

In spite of its importance, the Tuwaiq Mountain Formation is understudied compared to other Jurassic formations (e.g. Arab Formation).

1.4.1 Sedimentological and stratigraphical studies

The Tuwaiq Mountain Formation was formally defined by Bramkamp and Steineke (Arkell et al., 1952), and was described by Powers et al. (1966) and Powers (1968) who divided it into upper and lower units. Later, BRGM (Bureau de Recherches Géologiques et Minières) group divided the Tuwaiq Mountain Formation into three units T1, T2, and T3 which are informally named Baladiyah, Maysiyah, and Daddiyah members (Manivit et al., 1985; Vaslet et al., 1988; Vaslet et al., 1991; Énay et al., 2009). Recently, two members

(Hisyan and Atash Members of Dhruma Formation) were added to the Tuwaiq Mountain Formation (Hughes, 2009).

1.4.2 Paleontological and ichnological studies

Many paleontological studies have investigated the Tuwaiq Mountain Formation for its fossil content [Algal microfacies (Okla, 1987), Corals (El-Asa'ad, 1989), Ammonites (El-Asa'ad, 1992), Gastropods (Fischer et al., 2001), Benthic Foraminifera in Coral Reefs (Youssef & El-Sorogy, 2015)]. Micropaleontological characteristics of selected Jurassic unconformities (including Dhruma-Tuwaiq Mountain and Tuwaiq Mountain – Hanifa unconformities) have been discussed by Meyer & Hughes (2000). Hughes (2004, 2008, & 2009) conducted palaeoenvironmental interpretation of the major microfossil and selected macrofossil components of the Shaqra group (Figure 7: Hughes, 2004). El-Hedeny et al. (2012) described and interpreted trace fossils recorded in the formation and determined their environmental significance.

1.4.3 Geomorphological study

Only one study (Rausch et al., 2014) described the distribution of Tuwaiq Escarpment and its different geomorphologic features; gorges, spurs, buttes, and pinnacles.

1.4.4 Diagenetic study

A petrographic study, utilizing polarized microscope, of Jurassic Tuwaiq limestone rocks was conducted by Dabbagh (2006), who reported that lime mudstones and the wackestones constitute the bulk of Tuwaiq Mountain Formation while grainstone is less encountered and floatstone and boundstone are rare. Various diagenetic features were indicated in his study including cementation, micritization, dolomitization,

dedolomitization, and recrystallization. One of the most diagnostic diagenetic features to upper Tuwaiq, i.e. chertification, was not mentioned in this study.

In addition to identifying dolomite calcitization in the Tuwaiq Formation, Dabbagh (2006) described its different characteristic textures and proposed a mechanism of formation. His proposed mechanism was not supported by any evidence.

Discovering the origins and reconstructing the environment that produced any carbonate sequence are challenging tasks. As shown in the literature review, the biological (paleontological and ichnological studies) and physical (sedimentological and statigraphical studies) aspects have been covered by previous authors. However, the study of the physical and biological factors, if combined with the study of mineralogical and chemical factors can provide a more complete picture of the sedimentary depositional environment. There is a lack of geochemical and mineralogical studies in this formation.

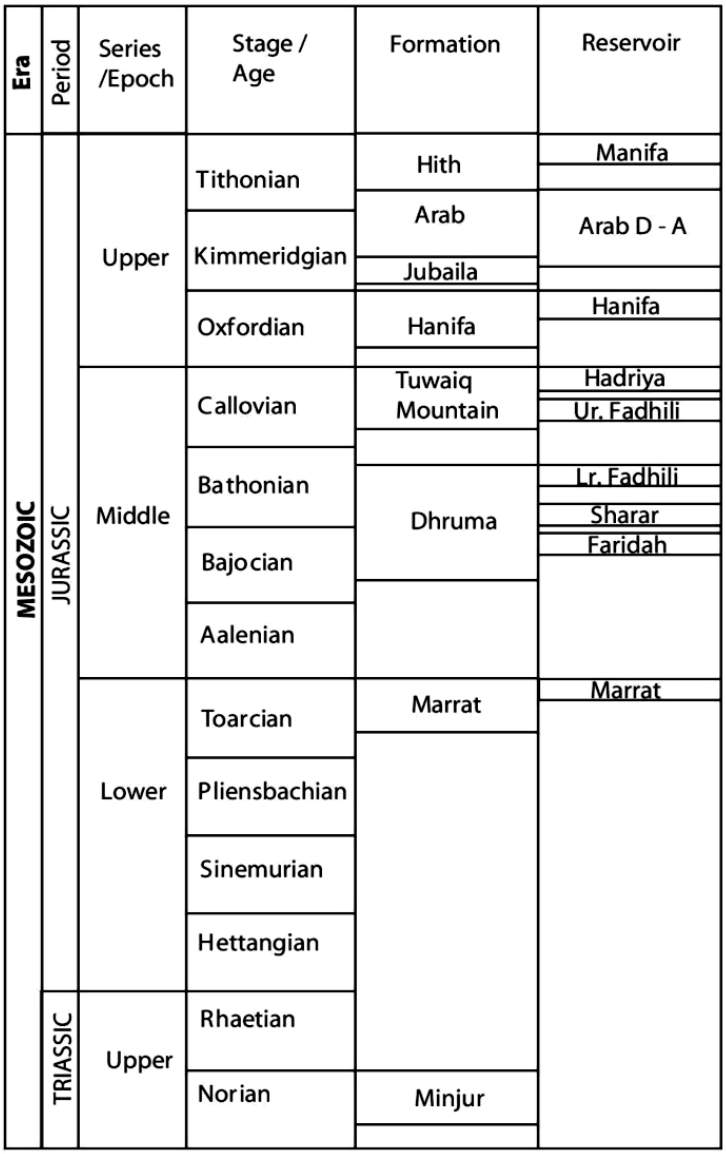

Figure 4. Lithostratigraphy and chronostratigraphy of members of the Shaqra Group of Saudi Arabia (Hughes, 2008).

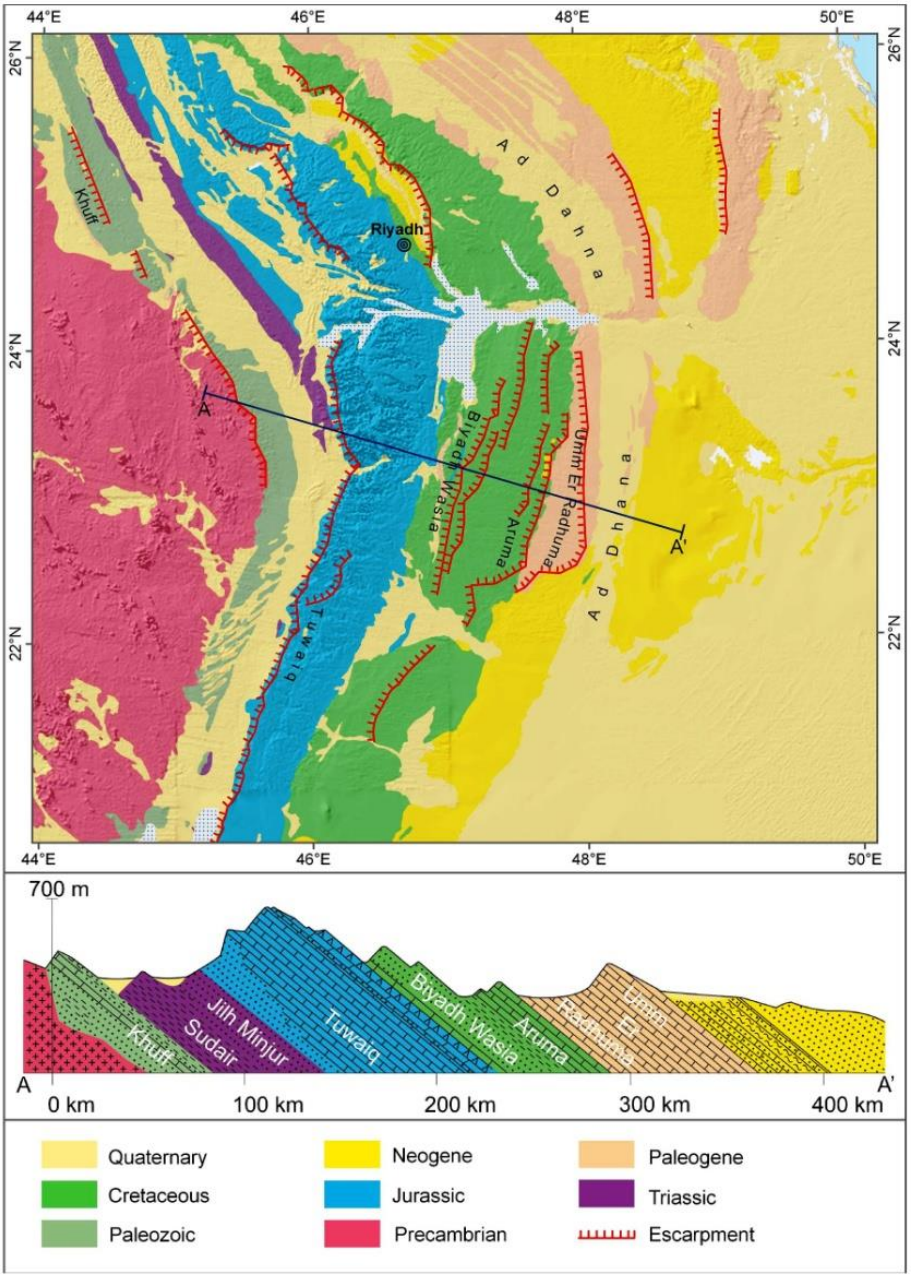

Figure 5. Geologic map and cross section showing the escarpments in the central part of Saudi Arabia (Rausch et al., 2014).

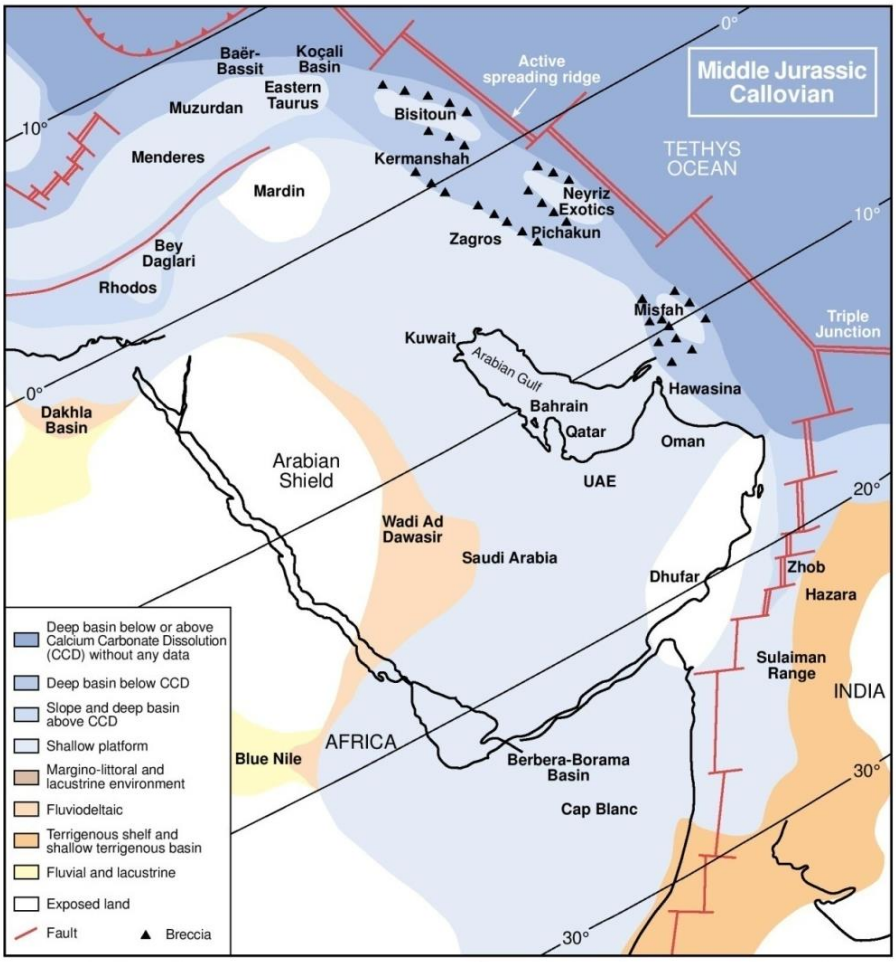

Figure 6. Paleoenvironment and tectonic reconstruction of the Middle Jurassic, Callovian. During the Callovian the upper Dhruma and Tuwaiq Mountain formations were deposited (Al-Husseini, 1997).

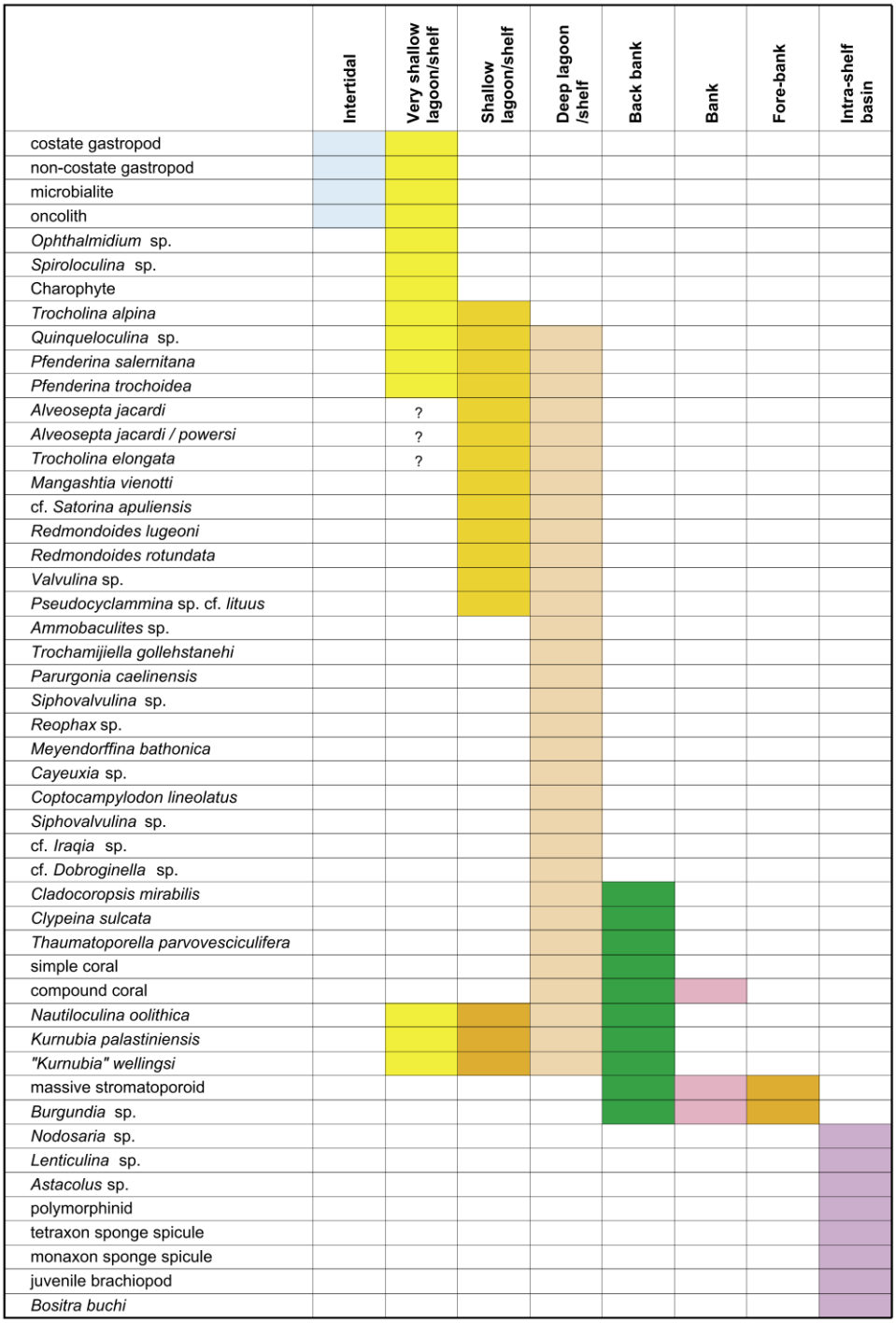

Figure 7. Suggested palaeoenvironmental model for Middle to Late Jurassic biocomponents (Hughes, 2004).

1.5 Objectives

The objectives of this study are listed below;

1) To report the distribution of dedolomites in Tuwaiq Mountain Formation.

2) To describe the dedolomites' petrographic characteristics.

3) To discuss the timing of dedolomitization relative to other diagenetic processes.

4) To suggest the source of the calcium-rich solution necessary for the dedolomitization reaction.

1.6 Thesis outline

This thesis consists of five chapters. Chapter one answers the following questions; why did I choose this area of research? Why did I choose Tuwaiq Mountain as a study area? Chapter two answers the following questions; which methods did I utilize in this study? Why did I choose them? How did I use them to get the results? Chapter three answers the following question; what did I find? Chapter four answers the following questions; what do the findings mean? What are the implications of these findings? Chapter five concludes my findings and my interpretation to these findings, and proposes some recommendations for future work.

CHAPTER 2 METHODOLOGY

2.1 Field Work

I have been to the field with my advisor four times [February 22-23, 2015, May 3-4, 2015, August 27-28, 2015, and December 4-5, 2015]. During these field trips we focused on logging the section and collecting samples. We documented our field observations especially those related to diagenesis. We collected representative samples needed for the purpose of my study.

2.1.1 Study area

Because of the difficulty to access the Tuwaiq Mountain Escarpment, we selected a road cut cutting through the formation. The outcrop succession examined in this study (Figures 8, 9) is a roadcut located along the Riyadh-Makkah highway, west of Riyadh [24°31'42.2"N 46°23'41.3"E].

2.1.2 Sampling strategy

Seventy samples (carbonates and cherts) were collected from the studied section. The sampling covered the whole road outcrop (encompassing units T1, T2, & T3) but sampling resolution was increased in the upper part (T3) where the chertification and dolomite calcitization have been reported in the previous studies (e.g. Vaslet et al., 1991; Dabbagh, 2006). While sampling interval for T1 and T2 was 3 m, it was 2 m for T3. Photos for the whole section and for the position of each sample were taken (Figures 9, 10). To label the samples, I utilized the following labeling system: OAR (represents my name's initials)-15 (represents the year in which the samples were collected)-0X (represents the number of the sample).

Figure 8. Satellite image showing an overview of study area. The study area is located at Khashm al Qaddiyah, west of Riyadh (24°31'42.2"N 46°23'41.3"E). Image provided from KACST, acquired on 16 October, 2014.

Figure 9. View of the Highway 40 road cut, looking east.

Figure 10. Sample 48's location, from the upper dark grey bed.

2.2 Laboratory Work

Different techniques that have been utilized to analyze the samples will be discussed in this section (Table 1).

2.2.1 Polarized Microscope (PM)

Examination using polarized microscope [Olympus EX51] (Figure 11) was conducted on thin sections injected with blue-dyed epoxy to easily recognize the pore spaces. One half of each thin section was stained with alizarin red-S to differentiate between calcite and dolomite. The study of the thin sections (68 samples) utilizing polarized microscope provides information about carbonate components, porosity types, texture types, and dedolomite presence.

2.2.2 Scanning Electron Microscope - Energy Dispersive X-Ray Spectrometer (SEM-EDS)

Examination using SEM-EDS [JEOL 6610 LV- Oxford X-Max^N Silicon Drift Detector] (Figure 12) was conducted on gold coated one cubic centimeter chips. The study of 25 samples provided information about crystals' habit, dedolomites' texture types, and elemental composition.

2.2.3 Inductively Coupled Plasma-Optical Emission Spectrometer (ICP-OES)

Examination using ICP-OES [SPECTRO CIROS VISION] (Figure 13) was conducted on 15 powdered bulk samples. One gram of the powders were weighed and placed in vials of 20 ml filled with 20 ml (5 %) HNO_3 and left reacting for two hours. ICP-OES was utilized to detect variation in some trace elements (e.g. Na, Fe) with the change in depth.

2.2.4 X-Ray Diffraction (XRD)

Examination using XRD [Rigaku Ultima IV] (Figure 14) was conducted on powdered bulk samples. Identification of the mineral content for 25 samples were conducted utilizing XRD. If there was more than one mineral in the sample, the relative concentration of each mineral was calculated.

2.2.5 Automated Porosimeter-Permeameter (APP)

Measurements of porosity and permeability (Figure 15) were conducted on 25 one-inch core plugs that were cut using the core plug drill machine. Porosity and permeability values were measured using Automated Porosimeter-Permeameter [AP-608].

Table 1. The collected samples and techniques utilized for analysis of the Carbonate samples (1-61) and Chert samples (67-69).

#	PM	SEM	XRD	XRF	ICP_OES	APP
OAR-15-001(Top)						
OAR-15-002						
OAR-15-003						
OAR-15-004						
OAR-15-005						
OAR-15-067						
OAR-15-006						
OAR-15-007						
OAR-15-008						
OAR-15-009						
OAR-15-010						
OAR-15-011						
OAR-15-012						
OAR-15-068						
OAR-15-013						
OAR-15-014						
OAR-15-015						
OAR-15-016						
OAR-15-069						
OAR-15-017						
OAR-15-018						
OAR-15-019						
OAR-15-020						
OAR-15-021						
OAR-15-022						
OAR-15-023						
OAR-15-024						
OAR-15-025						
OAR-15-026						
OAR-15-027						
OAR-15-028						
OAR-15-029						
OAR-15-030						
OAR-15-031						
OAR-15-032						
OAR-15-033						
OAR-15-034						
OAR-15-035						
OAR-15-036						
OAR-15-037						
OAR-15-038						

#	PM	SEM	XRD	XRF	ICP_OES	APP
OAR-15-039						
OAR-15-040						
OAR-15-041						
OAR-15-042						
OAR-15-043						
OAR-15-044						
OAR-15-045						
OAR-15-046						
OAR-15-047						
OAR-15-048						
OAR-15-049						
OAR-15-050						
OAR-15-051						
OAR-15-052						
OAR-15-054						
OAR-15-055						
OAR-15-056						
OAR-15-057						
OAR-15-058						
OAR-15-059						
OAR-15-060						
OAR-15-061(Bottom)						

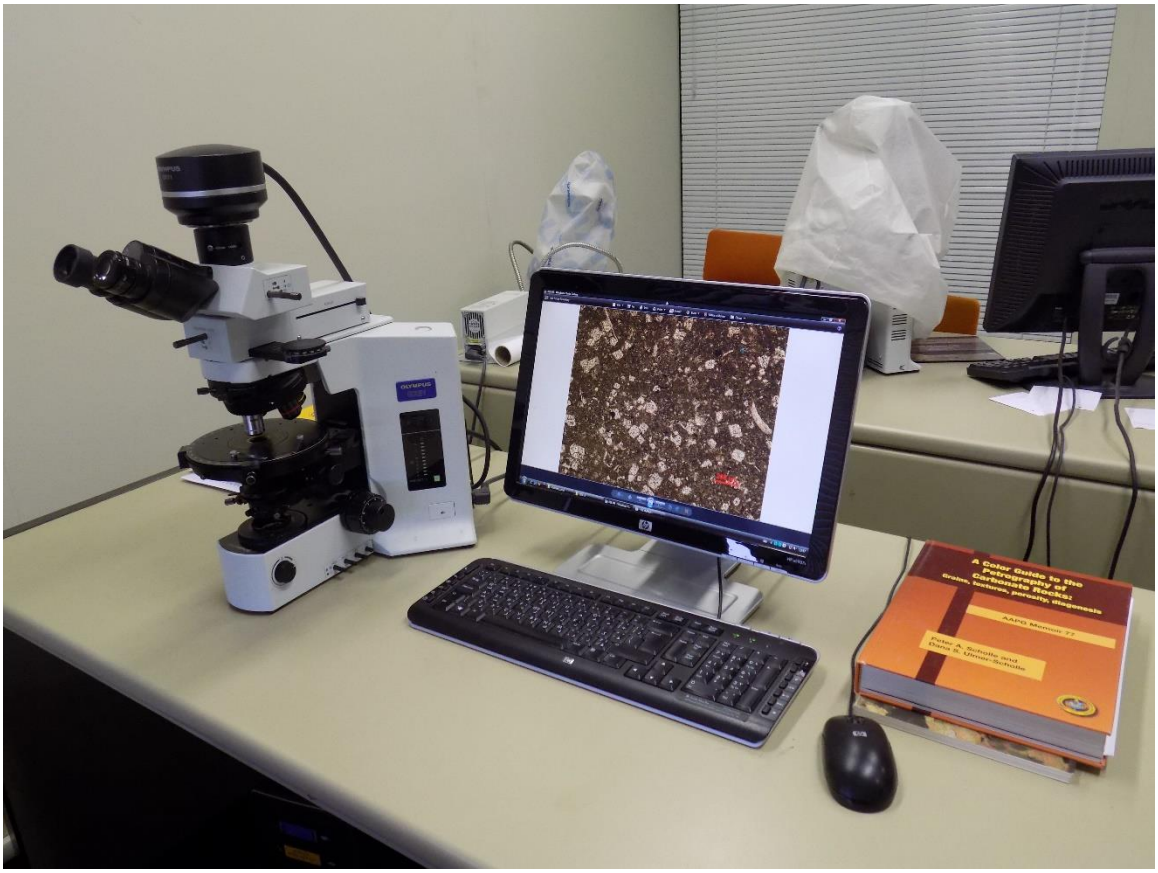

Figure 11. Polarized Microscope (PM) – Model: Olympus EX51 - Location: Building 15 Room 6134.

Figure 12. Scanning Electron Microscope - Energy Dispersive X-Ray Spectrometer (SEM-EDS) Model: JEOL 6610 LV- Oxford X-Max^{N} Silicon Drift Detector – Location: Building 15 Room 2203.

Figure 13. Inductively Coupled Plasma-Optical Emission Spectrometer (ICP-OES) – Model: SPECTRO CIROS VISION- Location: Building 15 Room 4217.

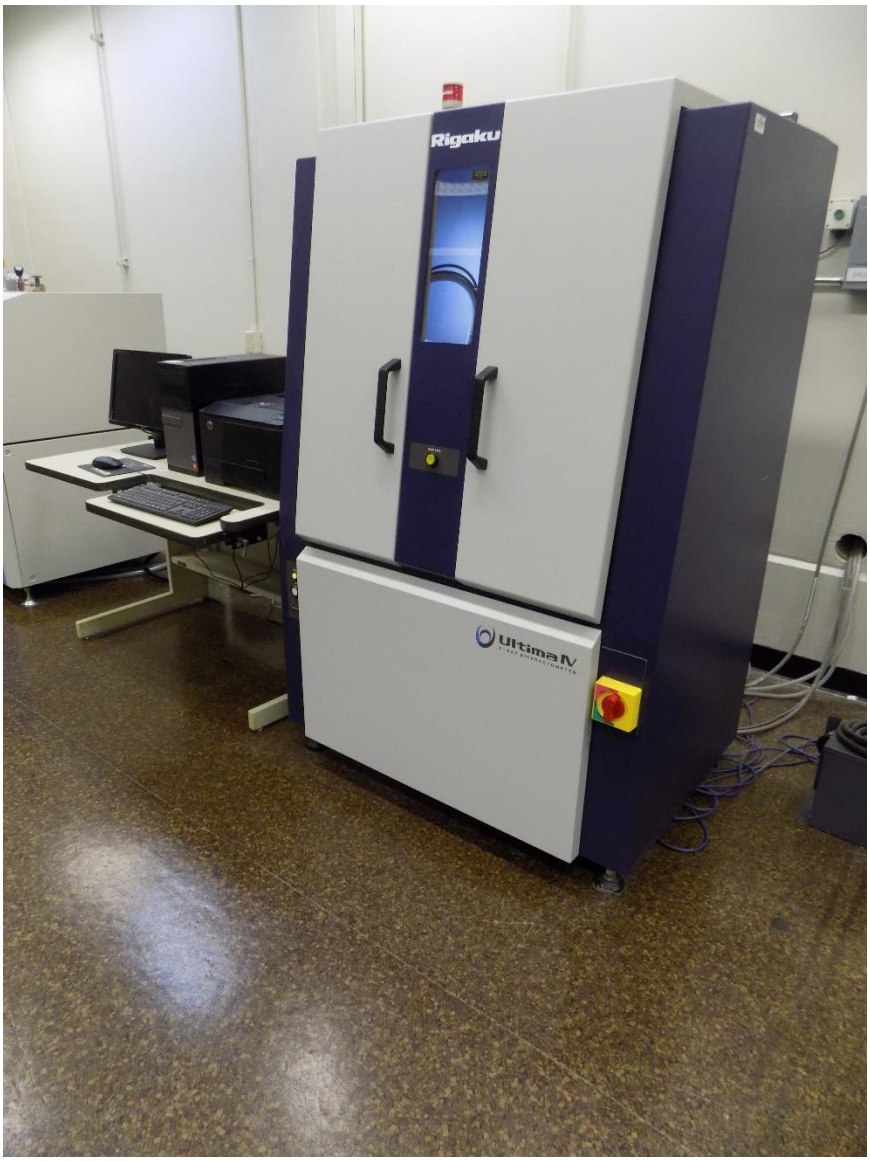

Figure 14. Powder X-Ray Diffraction (XRD) – Model: Rigaku Ultima IV - Location: Building 15 Room 2215.

Figure 15. Automated Porosimeter-Permeameter – Model: AP-608 - Location: Building 15 Room 6217.

CHAPTER 3 RESULTS

3.1 Field observations

The Tuwaiq Formation cliff is facing west. The thickness of the Tuwaiq Mountain Formation in the study area is about 180 m. The upper part is thicker than the middle and the lower parts (Figure 9).

The most prominent microfacies in the Tuwaiq Mountain limestone rocks are mudstone, wackestone, and packstone. Grainstone is less frequently encountered, and floatstone and boundstone are rare. The lower and upper part is, however, grainier than the middle part.

While few limestone units of the lower part are partly dolomitized, the middle and upper part contains calcite geodes infilling dissolution cavities (Figure 16). The middle part is characterized, in its upper part, by two dark grey beds (Figure 17). The upper part is characterized by a succession of prograding stromatoporoid bioherms (Figure 18). In the uppermost part, chert nodules occur at three horizons within the light yellow limestones (Figure 19). Horizon C (the lower) is grey colored and exhibits lenticular shape with maximum thickness of 10 cm. Horizon B (the middle) is white colored and exhibits lenticular shape with maximum thickness of 35 cm. Horizon A (the upper) is grey colored and exhibits lenticular shape with maximum thickness of 20 cm. Horizon A consists of many lenses stacked on each other. The density of nodular cherts increases toward the top.

Figure 20 shows simplified stratigraphic section of the Khashm Al-Qaddiyah section. Location of the section in Figure 8.

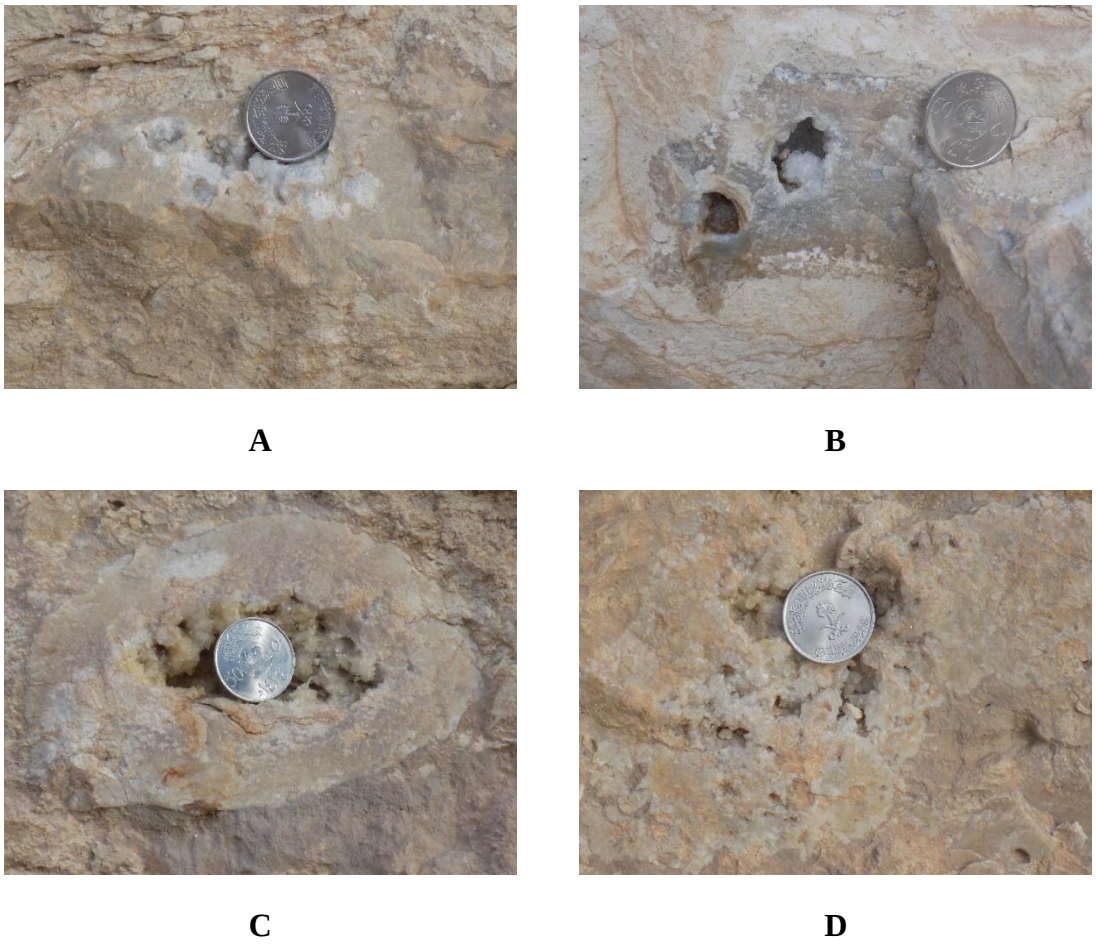

A **B**

C **D**

Figure 16. Calcite geodes filling dissolution cavities in the middle and upper part of the formation. **A-B**: calcite geodes in the middle part. **C-D**: calcite geodes in the upper part.

Figure 17. The dark grey mudstone beds within the middle part.

Figure 18. The upper part is characterized by a succession of prograding stromatoporoid bioherms.

A

B

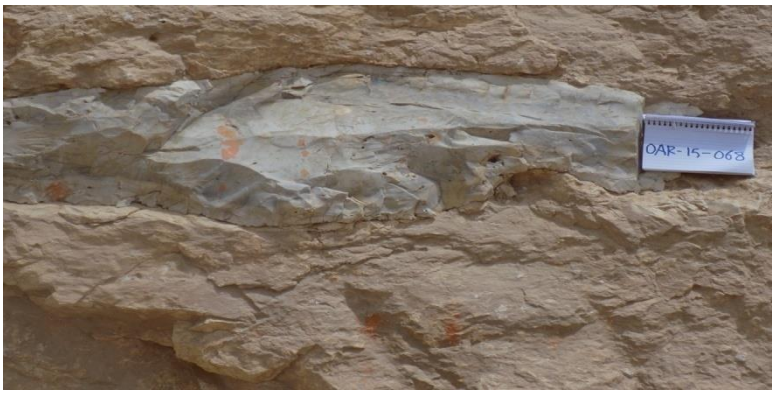

C

Figure 19. Chert nodules occur at three horizons (from Top to bottom: **A-B-C**) within the light yellow limestones in the upper part of T3.

Era	Period	Epoch	Age	Supergroup	Group	Formation	Member	Sample #	Depth	Lithology
Mesozoic	Jurassic	Upper	Oxfordian	Dir'iyah	Shaqra	Hanifa	Hawtah		0 m	
		Middle	Callovian			Tuwaiq Mountain	T3 Daddiyah	01-40		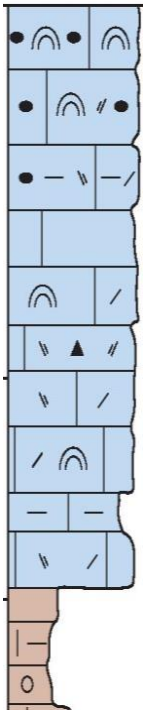
							T2 Maysiyah	40-50	100 m	
							T1 Baladiyah	50-60	150 m	
			Bathonian			Dhruma	Hisyan		180 m	

Figure 20. Simplified stratigraphic section of the studied area.

3.2 Petrography

As expected, lime mudstones and the wackestones constitute the bulk of the Tuwaiq Mountain Formation while grainstone is less frequently encountered. Table 2 shows the Dunham classification of the samples based on the microscopic examination.

There are numerous microfabrics in the samples other than the ten microfabric types listed below, but only the microfabrics that are pertinent to dedolomitization process are discussed here.

3.2.1 **Microfabric Type-I**: Dolomite crystal

Description: isolated dolomite crystals scattered through muddy lime groundmass (Figure 21).

Distribution: this type of microfabric is concentrated in the lowermost part of the studied section.

3.2.2 **Microfabric Type-II**: Rhombohedral pores

Description: open rhombohedral pores either without (Figure 22-a) or with (Figure 22-b) calcite relicts around the rim.

Distribution: this type of microfabric is concentrated in the uppermost part of the studied section.

3.2.3 **Microfabric Type-III**: Single calcite crystal pseudomorph after dolomite [C-I]

Description: In most samples rhombohedral porosity has been destroyed by subsequent calcite cementation. Cementation shows a variety of textures (Figure 23-25). C-I stands for cementation texture number one. In C-I, single calcite rhombohedral crystal is occupying the rhombohedral pore (Figure 23).

Distribution: this type of microfabric is concentrated in the upper part of the studied section.

3.2.4 Microfabric Type-IV: Polycrystalline calcite pseudomorph after dolomite [C-II]

Description: The cementation is mostly polycrystalline (drusy texture). In this type of texture, rhombohedra vary in size from 150 to 200 μm (Figure 24). C-II stands for cementation texture number two.

Distribution: this type of microfabric is concentrated in the uppermost part of the studied section.

3.2.5 Microfabric Type-V: Pore-filling & Fracture-filling [C-III]

Description: cementation also exhibits pore-filling (Figure 25-a) and fracture-filling textures (Figure 25-b). C-III stands for cementation texture number three.

Distribution: this type of microfabric is concentrated in the uppermost part of the studied section.

3.2.6 Microfabric Type-VI: Polycrystalline calcite pseudomorph after dolomite [R]

Description: In other samples the dolomite was replaced by composite calcite rhombohedra (Figure 26). In this type of texture, rhombohedra vary in size from 20 to 50 μm. R stands for replacement texture.

Distribution: this type of microfabric is concentrated in the middle part of the studied section.

3.2.7 Microfabric Type-VII: Calcite pseudomorphs after lenticular gypsum

Description: polycrystalline calcite is filling lenticular molds formerly occupied by gypsum crystals (Figure 27).

Distribution: this type of microfabric is concentrated in the uppermost part of the studied section.

3.2.8 **Microfabric Type-VIII**: Microcrystalline quartz of chert

Description: microcrystalline quartz constitutes the bulk of the chert horizons and nodules (Figure 28).

Distribution: this type of microfabric is concentrated in the uppermost part of the studied section.

3.2.9 **Microfabric Type-IX**: Evaporite relicts within microcrystalline quartz of chert

Description: relicts of evaporite minerals were found within microcrystalline quartz of the cherts (Figure 29).

Distribution: this type of microfabric is concentrated in the uppermost part of the studied section.

3.2.10 **Microfabric Type-X**: Sponge spicules in the cherts and the carbonates

Description: An abundance of sponge spicules in the cherts (Figure 30-a) and surrounding carbonate (Figure 30-b) was observed.

Distribution: this type of microfabric is concentrated in the uppermost part of the studied section.

Table 2. Dunham classification of the samples based on microscopic examination. M: Mudstone, W: Wackestone, P: Packstone, MLP: Mud-Lean Packstone, G: Grainstone.

	Sample #	Dunham classification	M	W	P	MLP	G
Top	**OAR-15-001**	Packstone	■	■	■		
	OAR-15-002	Packstone	■	■	■		
	OAR-15-003	Wackestone	■	■			
	OAR-15-004	Grainstone	■	■	■	■	■
	OAR-15-005	Wackestone	■	■			
	Siliceous lenticular bed [067]						
	OAR-15-006	Wackestone	■	■			
	OAR-15-007	Wackestone	■	■			
	OAR-15-008	Wackestone	■	■			
	OAR-15-009	Wackestone	■	■			
	OAR-15-010	Wackestone	■	■			
	OAR-15-011	Wackestone	■	■			
	OAR-15-012	Wackestone	■	■			
	Siliceous lenticular bed [068]						
	OAR-15-013	Wackestone	■	■			
	OAR-15-014	Mudstone	■				
	OAR-15-015	Wackestone	■	■			
	OAR-15-016	Wackestone	■	■			
	Siliceous lenticular bed [069]						
	OAR-15-017	Packstone	■	■	■		
	OAR-15-018	Wackestone	■	■			
	OAR-15-019	packstone	■	■	■		
	OAR-15-020	Packstone	■	■	■		
	OAR-15-021	Wackestone	■	■			
	OAR-15-022	Wackestone	■	■			
	OAR-15-023	Wackestone	■	■			
	OAR-15-024	Packstone	■	■	■		
	OAR-15-025	Mudstone	■				
	OAR-15-026	Mudstone	■				
	OAR-15-027	Grainstone	■	■	■	■	■
	OAR-15-028	Wackestone	■	■			
	OAR-15-029	Packstone	■	■	■		
	OAR-15-030	Packstone	■	■	■		
	OAR-15-031	Packstone	■	■	■		
	OAR-15-032	Packstone	■	■	■		
	OAR-15-033	Wackestone	■	■			
	OAR-15-034	Wackestone	■	■			
	OAR-15-035	Wackestone	■	■			
	OAR-15-036	Packstone	■	■	■		
	OAR-15-037	Wackestone	■	■			

	Sample #	Dunham classification	M	W	P	MLP	G
	OAR-15-038	Packstone					
	OAR-15-039	Grainstone					
	OAR-15-040	Packstone					
	OAR-15-041	Packstone					
	OAR-15-042	Mud-Lean Packstone					
	OAR-15-043	Packstone					
	OAR-15-044	Wackestone					
	OAR-15-045	Wackestone					
	OAR-15-046	packstone					
	OAR-15-047	packstone					
	OAR-15-048	wackestone					
	OAR-15-049	Mudstone					
	OAR-15-050	Mudstone					
	OAR-15-051	Wackestone					
	OAR-15-052	Wackestone					
	OAR-15-053	Wackestone					
	OAR-15-054	Wackestone					
	OAR-15-055	Wackestone					
	OAR-15-056	Wackestone					
	OAR-15-057	Wackestone					
	OAR-15-058	Wackestone					
	OAR-15-059	Packstone					
	OAR-15-060	Packstone					
	OAR-15-061	Wackestone					
Bottom							

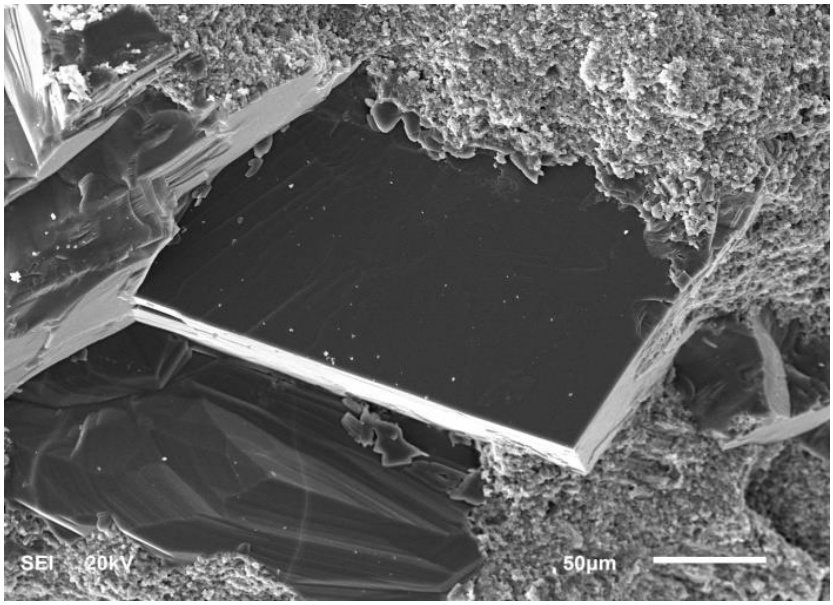

A

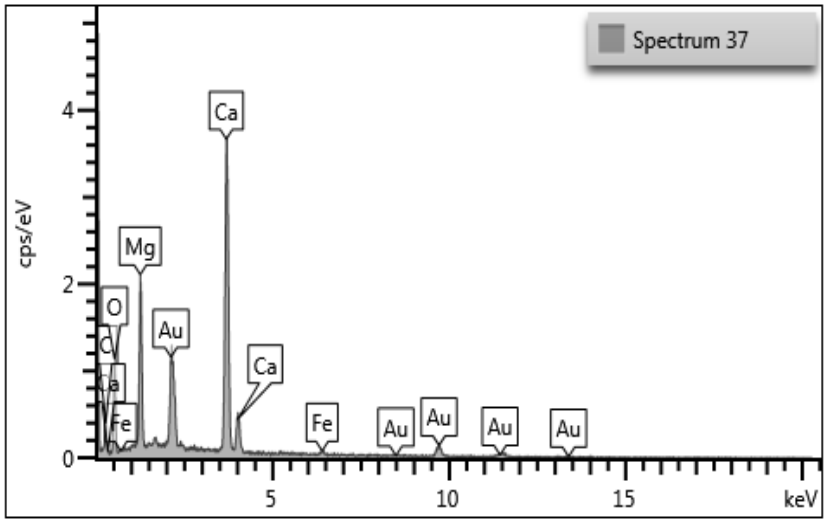

B

Figure 21. Microfabric type – I. **A)** Dolomite crystal from T1 (Sample: OAR-15-59). **B)** EDS data for the crystal in the center.

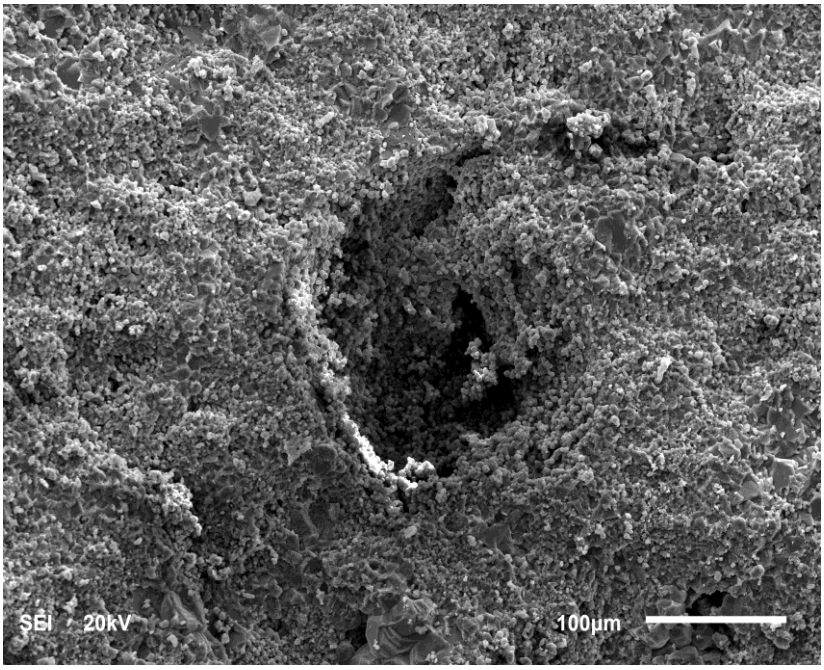

A

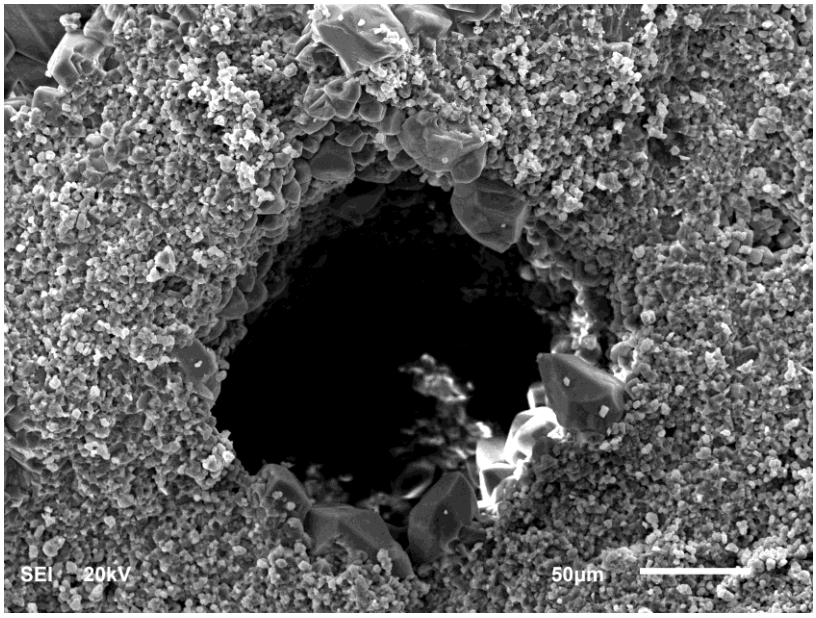

B

Figure 22. Microfabric type – II: Open rhombohedral pores either without (**A**) or with (**B**) calcite crystals along the rim.

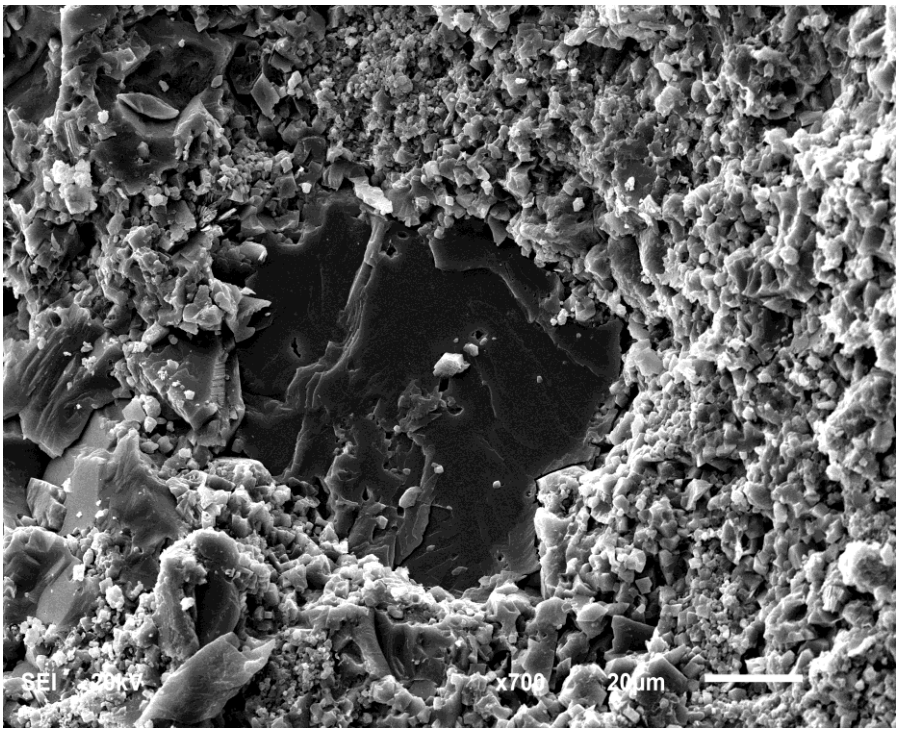

A

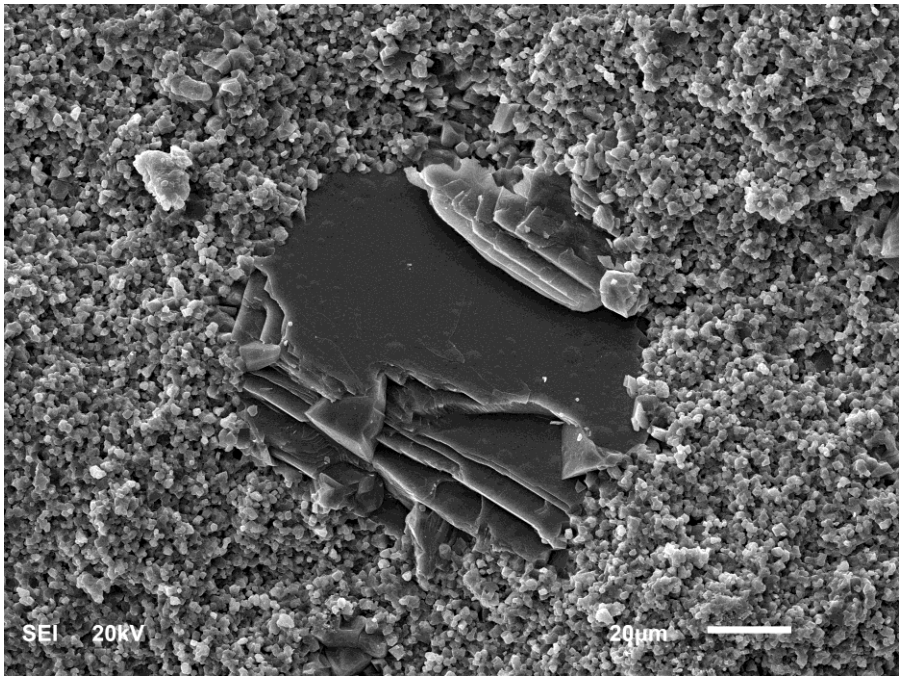

B

Figure 23. Microfabric type – III: Single calcite crystal pseudomorph after dolomite (**A-B**).

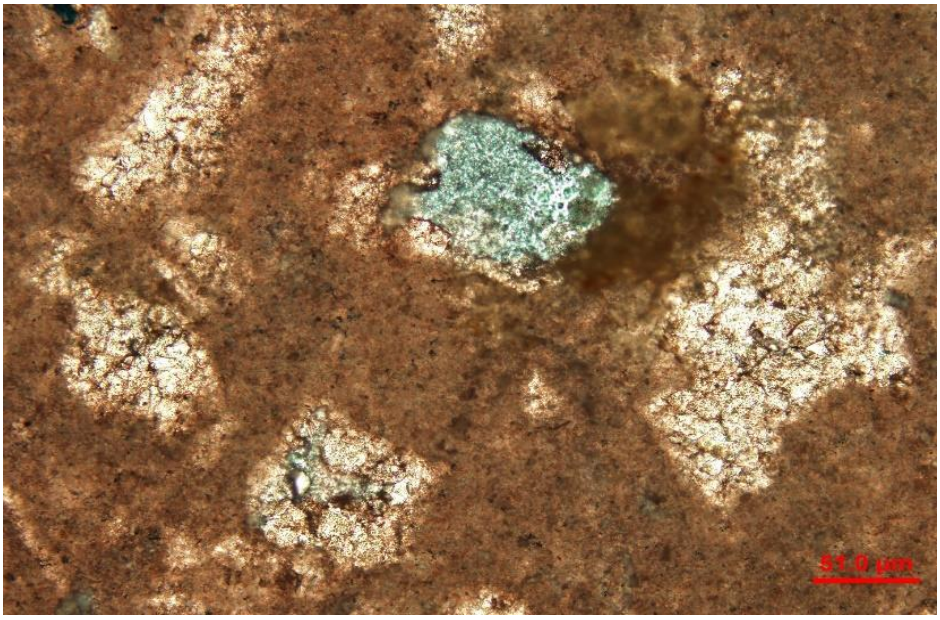

A

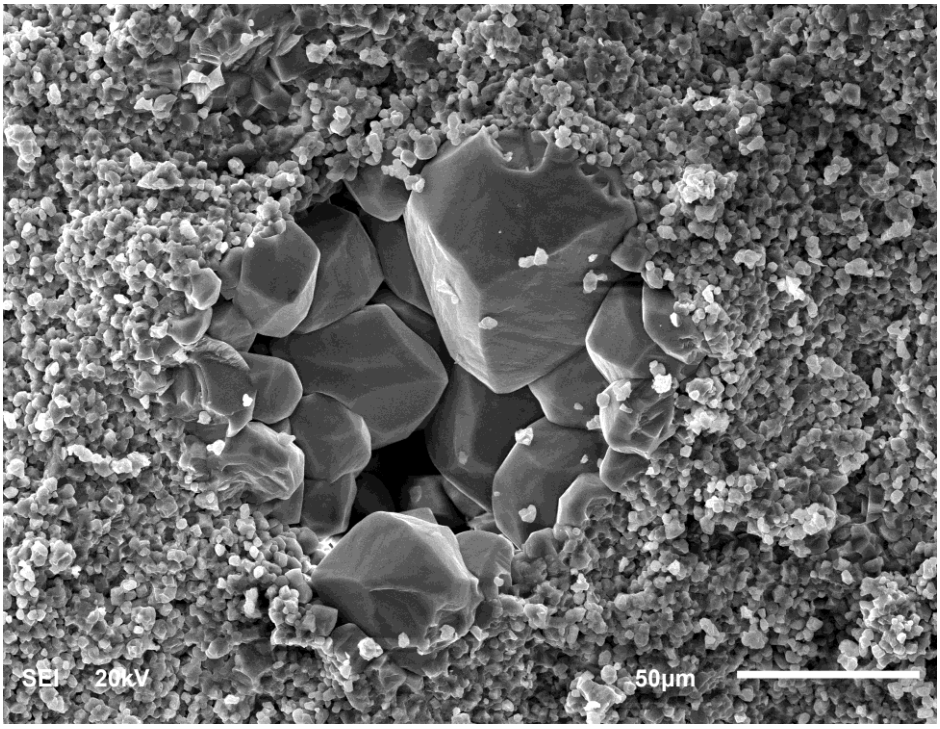

B

Figure 24. Microfabric type – IV: Polycrystalline calcite pseudomorph after dolomite. **A)** calcite crystals partially or completely filling the rhombohedral pores, view under polarized microscope. **B)** equant calcite crystals filling the rhombohedral pore, view under SEM.

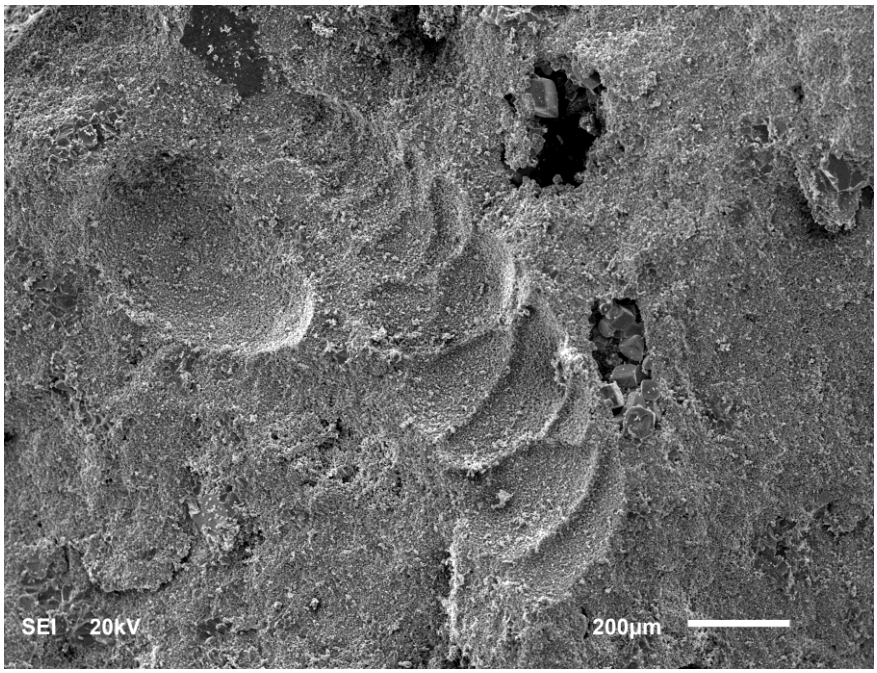

A

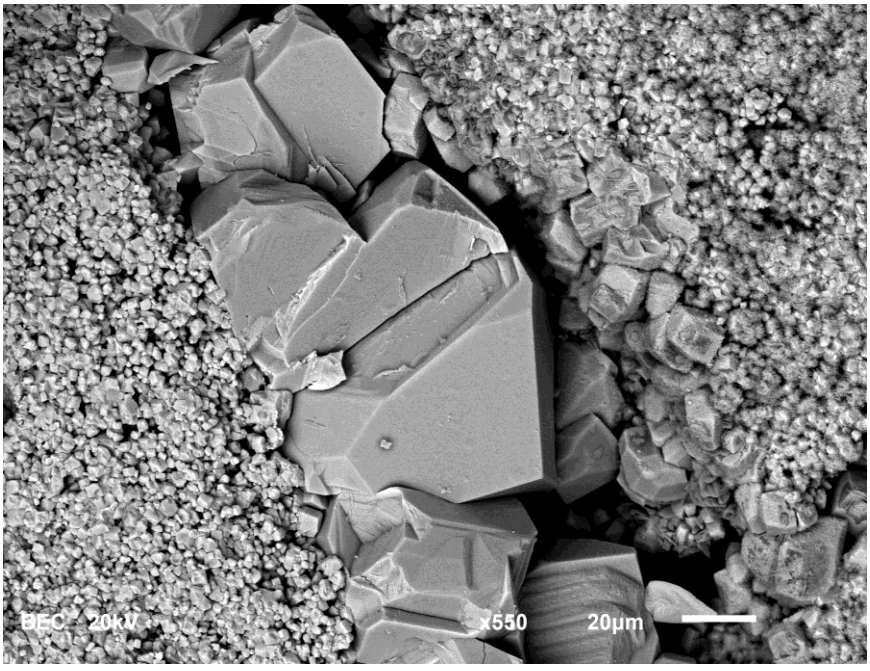

B

Figure 25. Microfabric type -V: Pore-filling & Fracture-filling textures. **A)** equant calcite crystals filling the pores beside the fossil imprint. **B)** platy to equant calcite crystals filling the fractures.

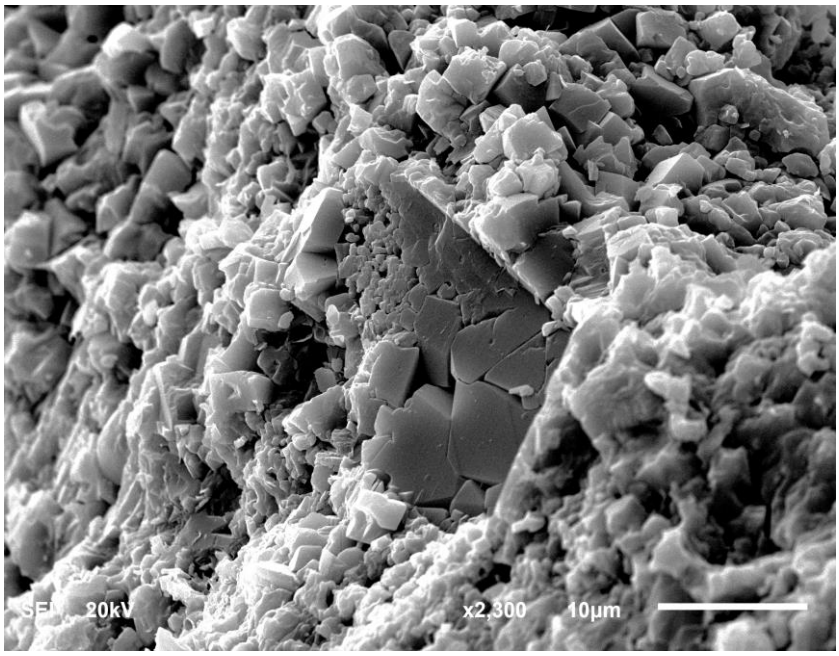

A

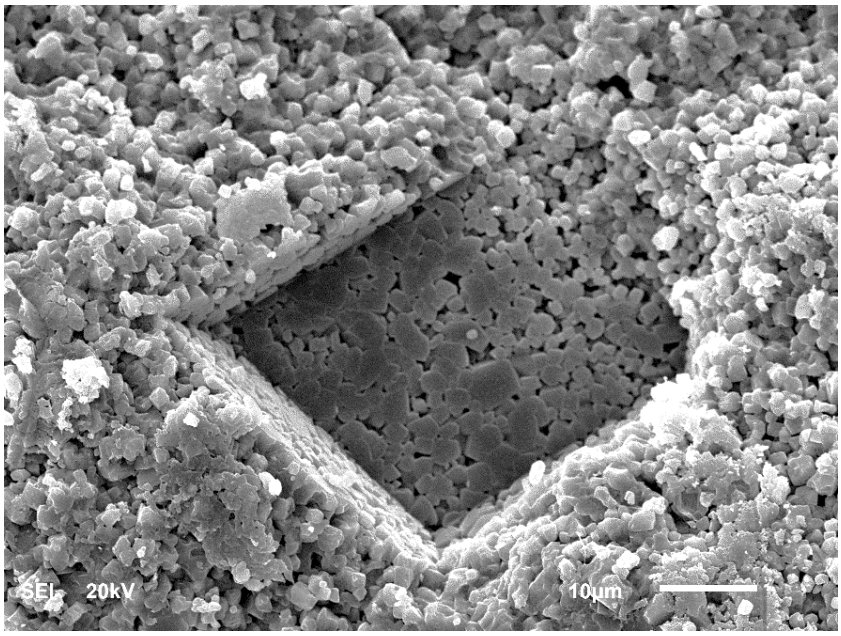

B

Figure 26. Microfabric type – VI: composite calcite rhombohedra replacing dolomite (**A-B**).

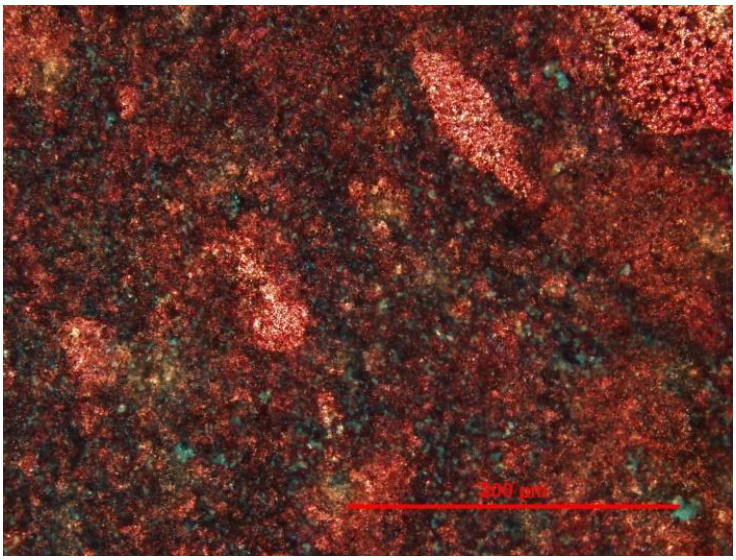

A

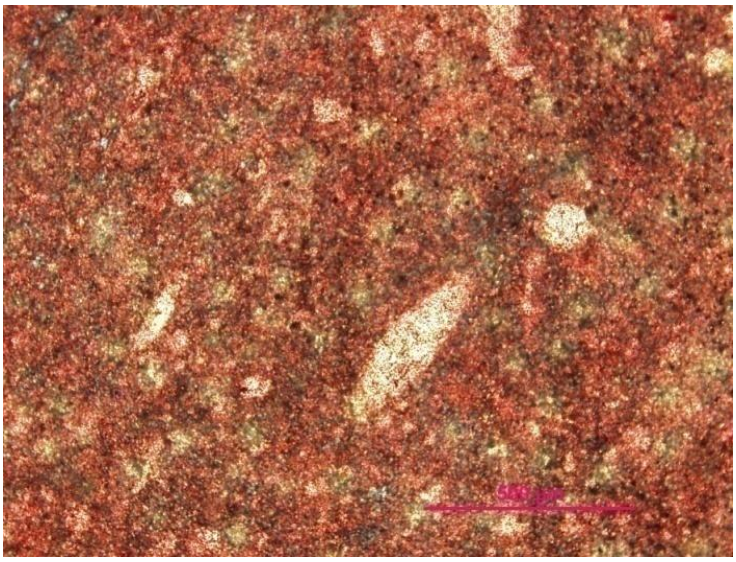

B

Figure 27. Microfabric type – VII: Calcite pseudomorphs after lenticular gypsum (**A-B**).

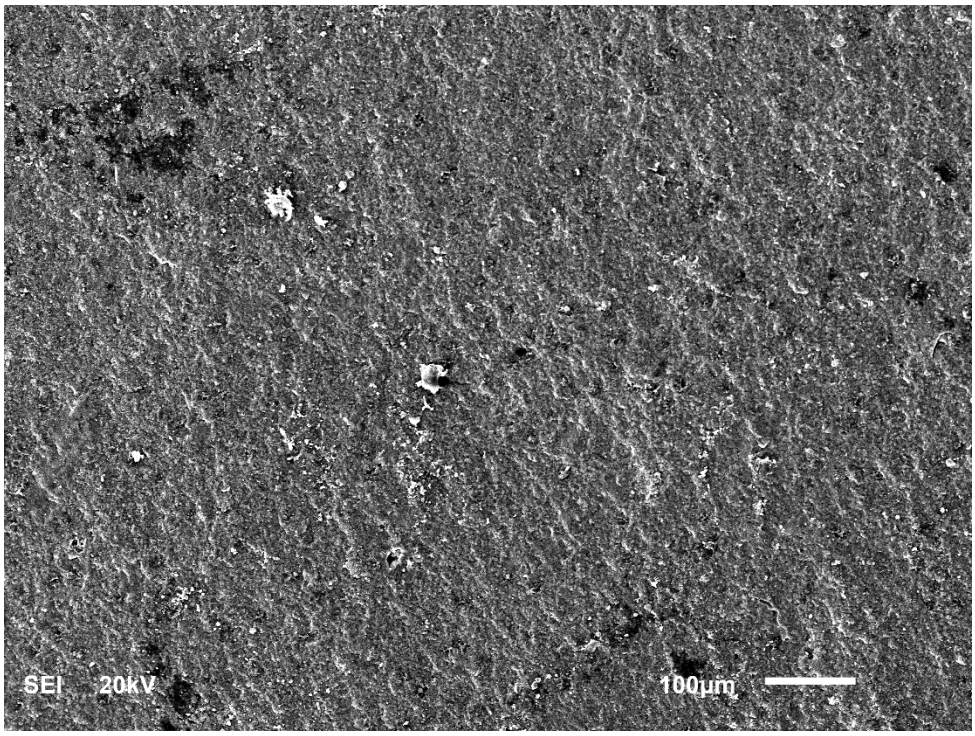

Figure 28. Microfabric type – -VIII: Microcrystalline quartz of chert.

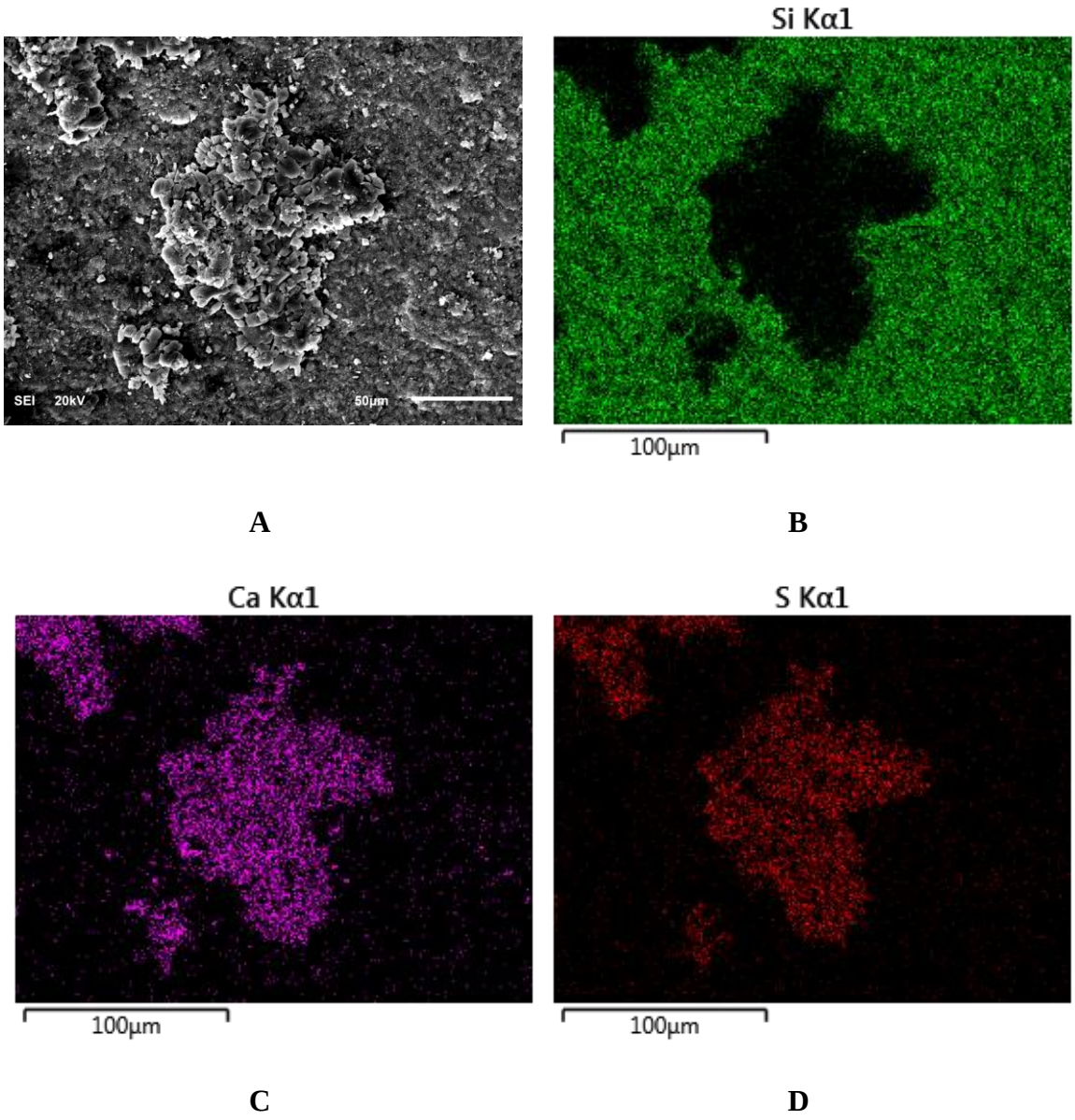

Figure 29. Microfabric type -IX: Evaporite relicts within microcrystalline quartz of chert. **A**) evaporite relicts in the siliceous background, view under SEM. Element distribution images (**B**, **C**, & **D**) for silicon, calcium, and sulphur respectively, view by EDS mapping.

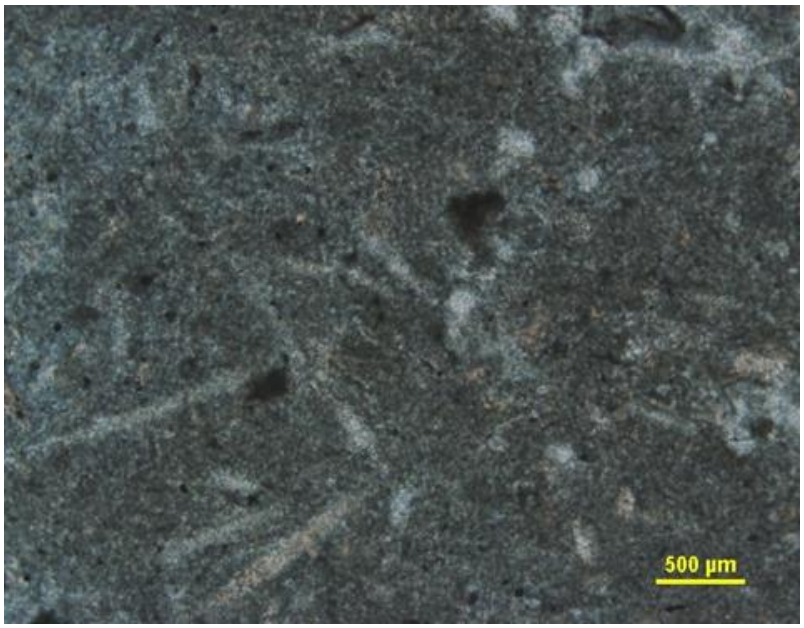

A

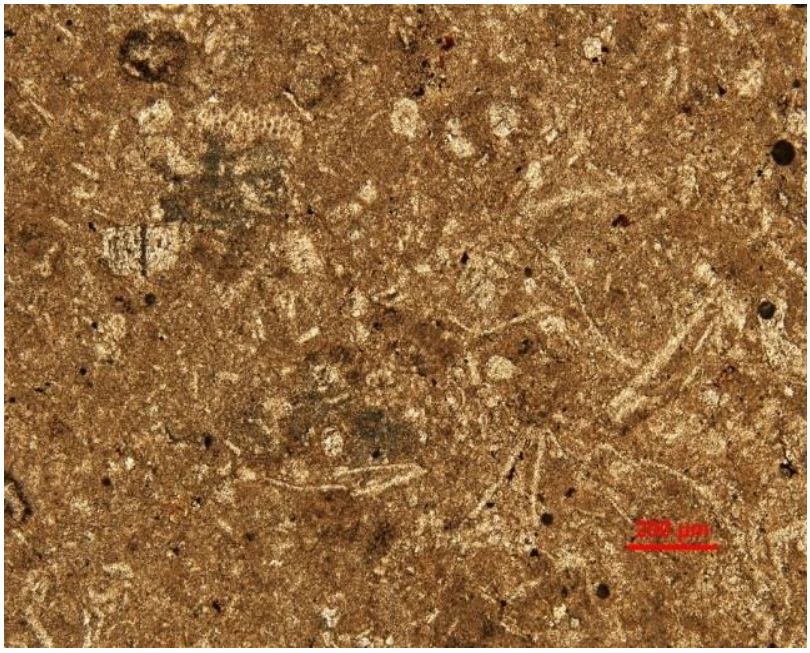

B

Figure 30. Microfabric type -X: abundance of sponge spicules in the cherts (**A**) and the surrounding carbonates (**B**).

3.3 Mineralogical composition

Most of the Tuwaiq Mountain carbonate samples (Figure 31) are monomineralic, i.e. formed of pure calcite. The quartz content in the carbonate samples increases in two horizons; around the chert nodules in the upper part (Figure 32-a) and in the dark grey layers in the middle part (Figure 32-b). In the lowermost part, another carbonate phase (dolomite) exists in low concentration. The dolomite concentration increases with depth (Figure 33).

The cherts are composed of microcrystalline quartz. X-ray diffraction analyses show that quartz is the only silica phase present in all samples (Figure 34).

3.4 Chemical composition

ICP-OES was utilized to detect the variation in trace element concentrations in the carbonate samples. There is a significant increase in iron, potassium, and aluminum amount in samples 48 (the dark grey bed). Topmost samples are poor in sodium and iron amount relative to the rest of the formation (Table 3).

3.5 Porosity and permeability

Porosities range from 10-12% in the middle and lower part of the studied section, while the porosity ranges from 5-20% in the upper part. Permeability values range from 0.04-0.3 mD in the middle and lower part of the studied section, while the permeability values range from 0.03-9 mD in the upper part. The wider range of porosity and permeability values of the upper part relative to the middle and lower parts is shown in table 4.

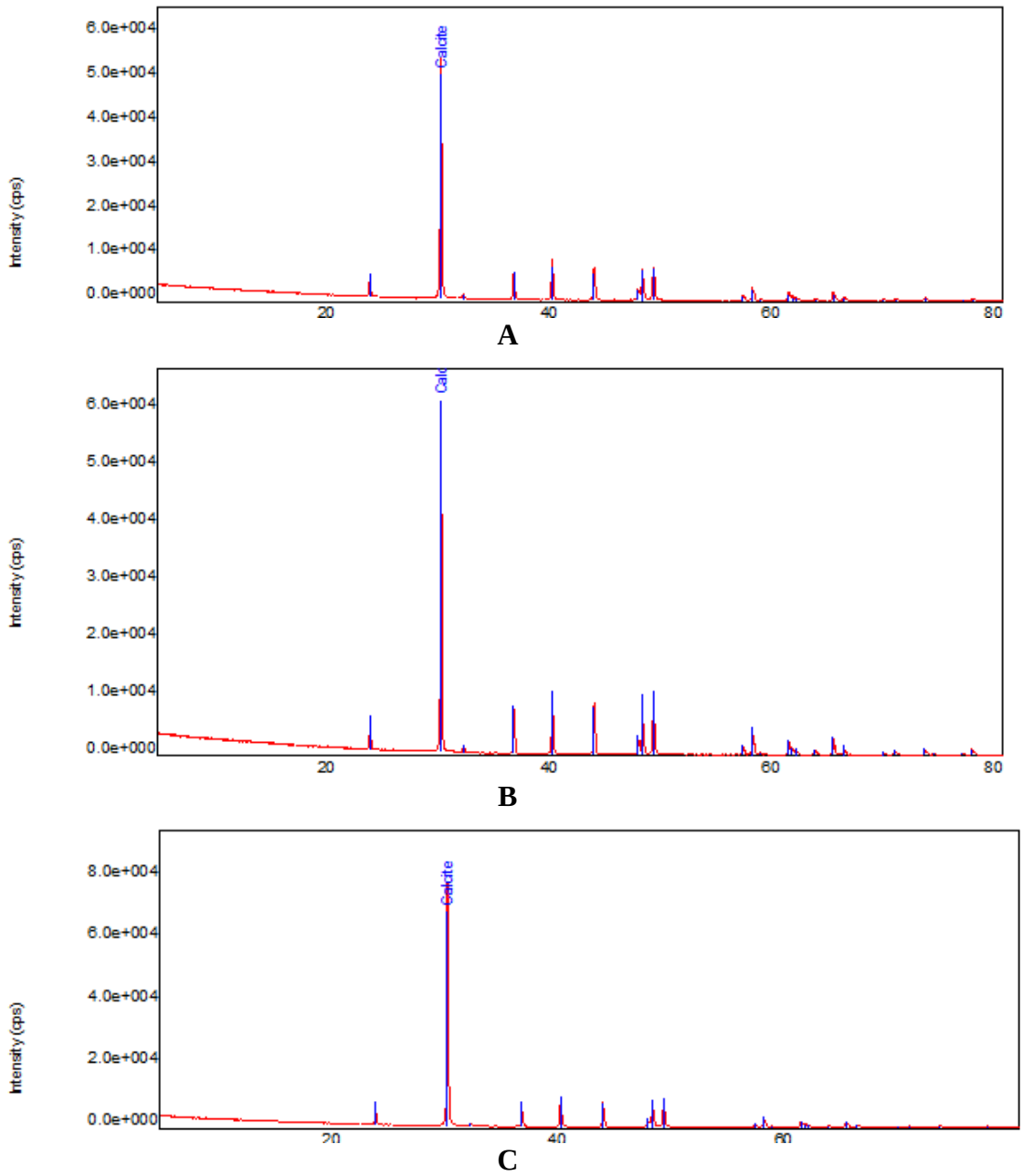

Figure 31. Most of the carbonate samples of the studied area are formed of calcite only. **A)** XRD pattern of sample # 02: 100 % calcite. **B)** XRD pattern of sample # 12: 100 % calcite. **C)** XRD pattern of sample # 22: 100 % calcite.

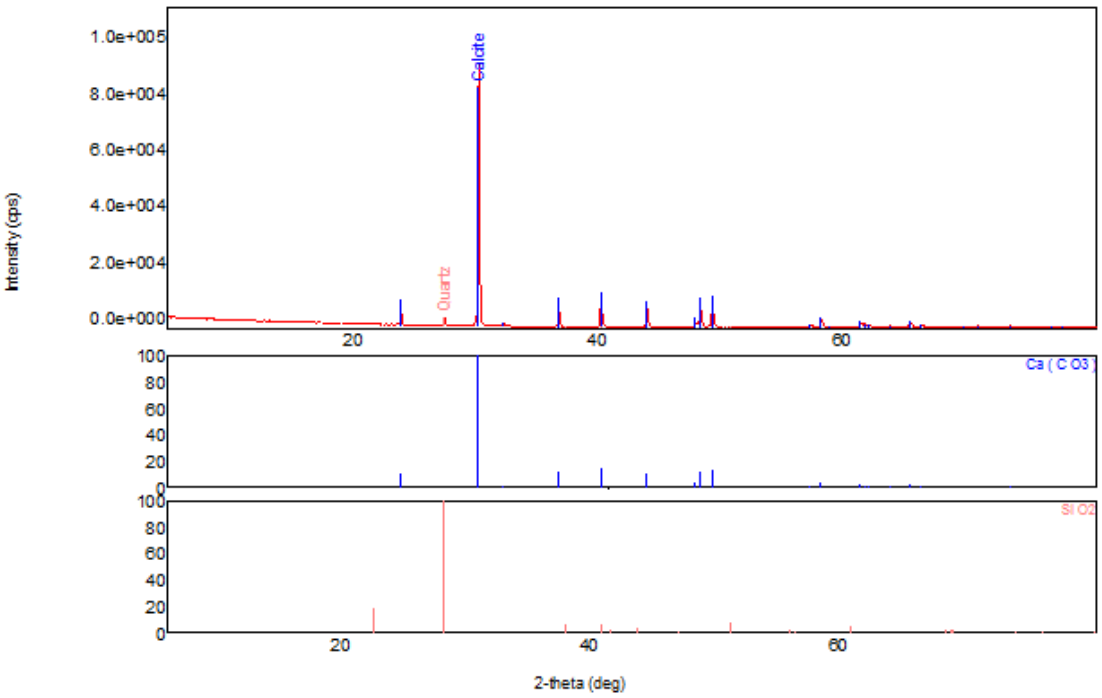

A

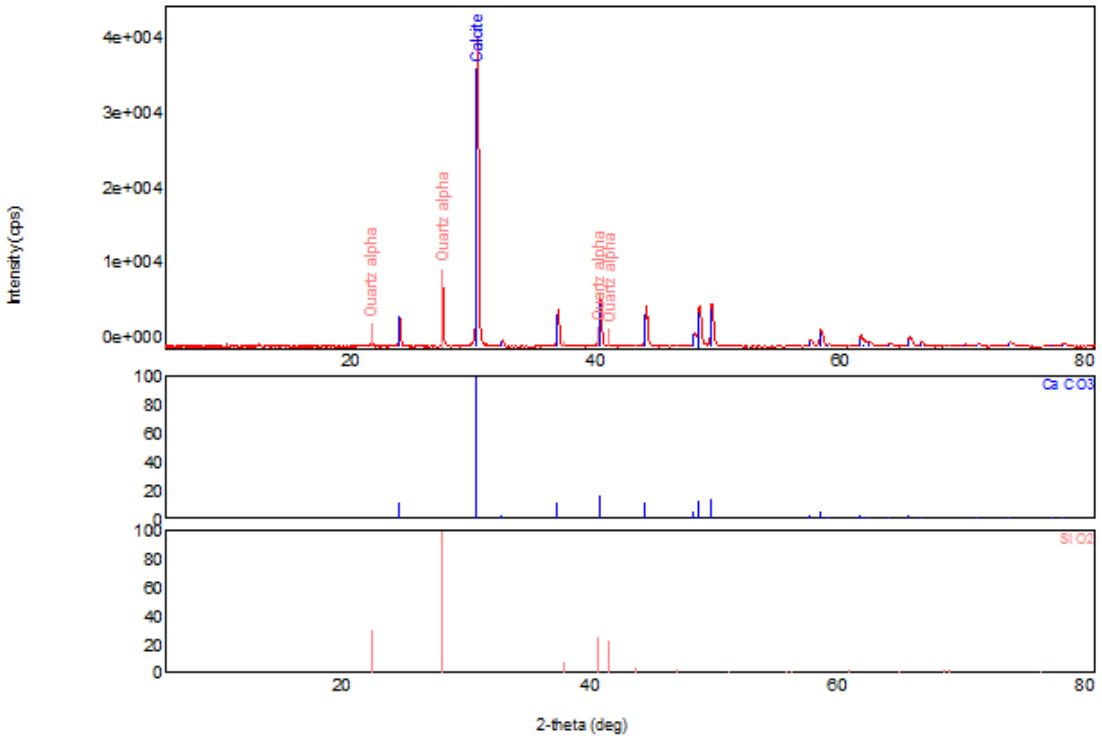

B

Figure 32. Some of the carbonate samples contain significant amount of quartz in the upper and middle parts. **A)** XRD pattern of sample # 08: 95.7 % calcite and 4.3 % quartz. **B)** XRD pattern of sample # 48: 83.7 % calcite and 16.3 % quartz.

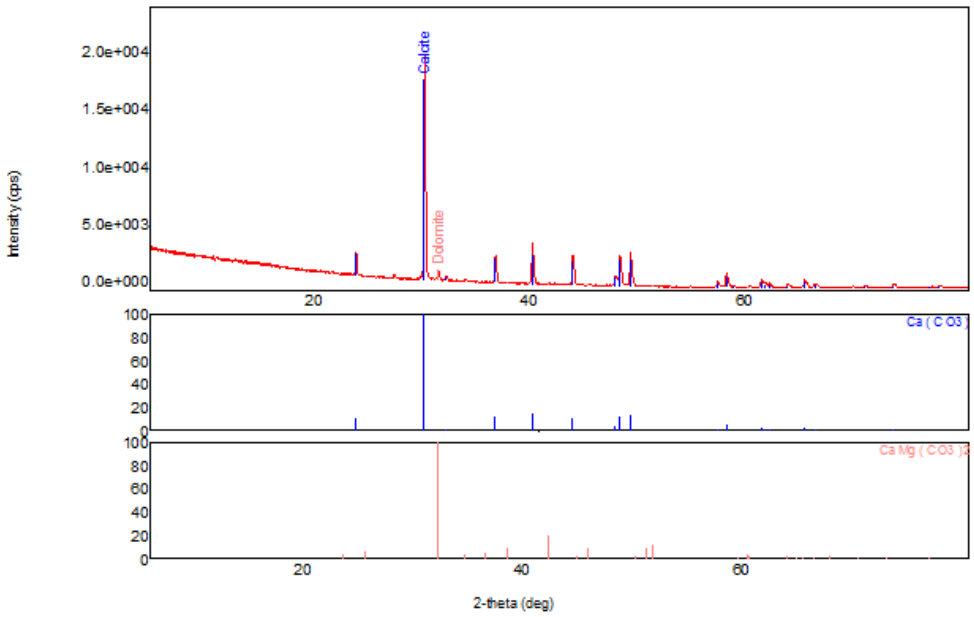

A

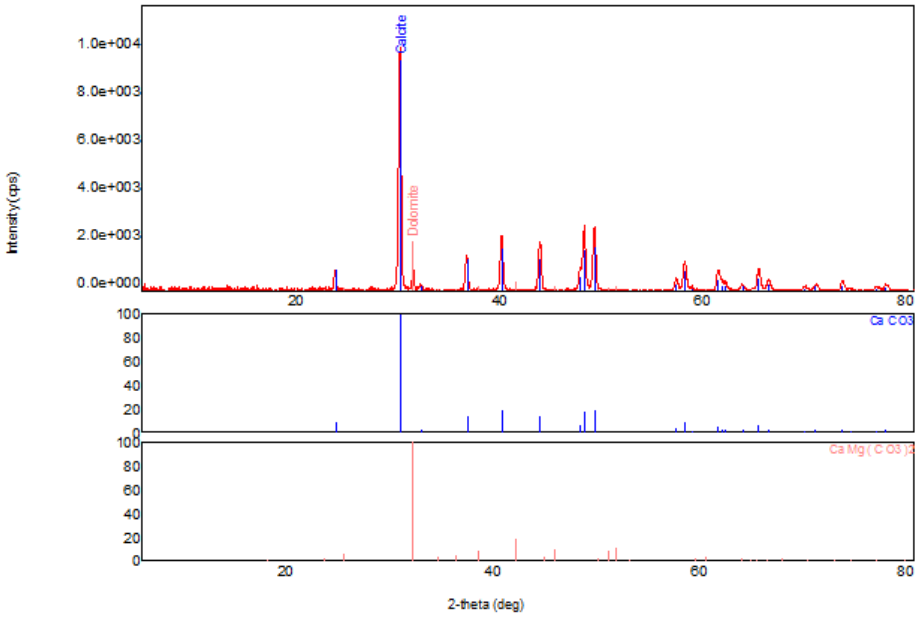

B

Figure 33. Dolomite concentration increases with depth. **A)** XRD pattern of sample # 54: 98.9 % calcite and 1.06 % dolomite. **B)** XRD pattern of sample # 58: 91.1 % calcite and 8.9 % dolomite.

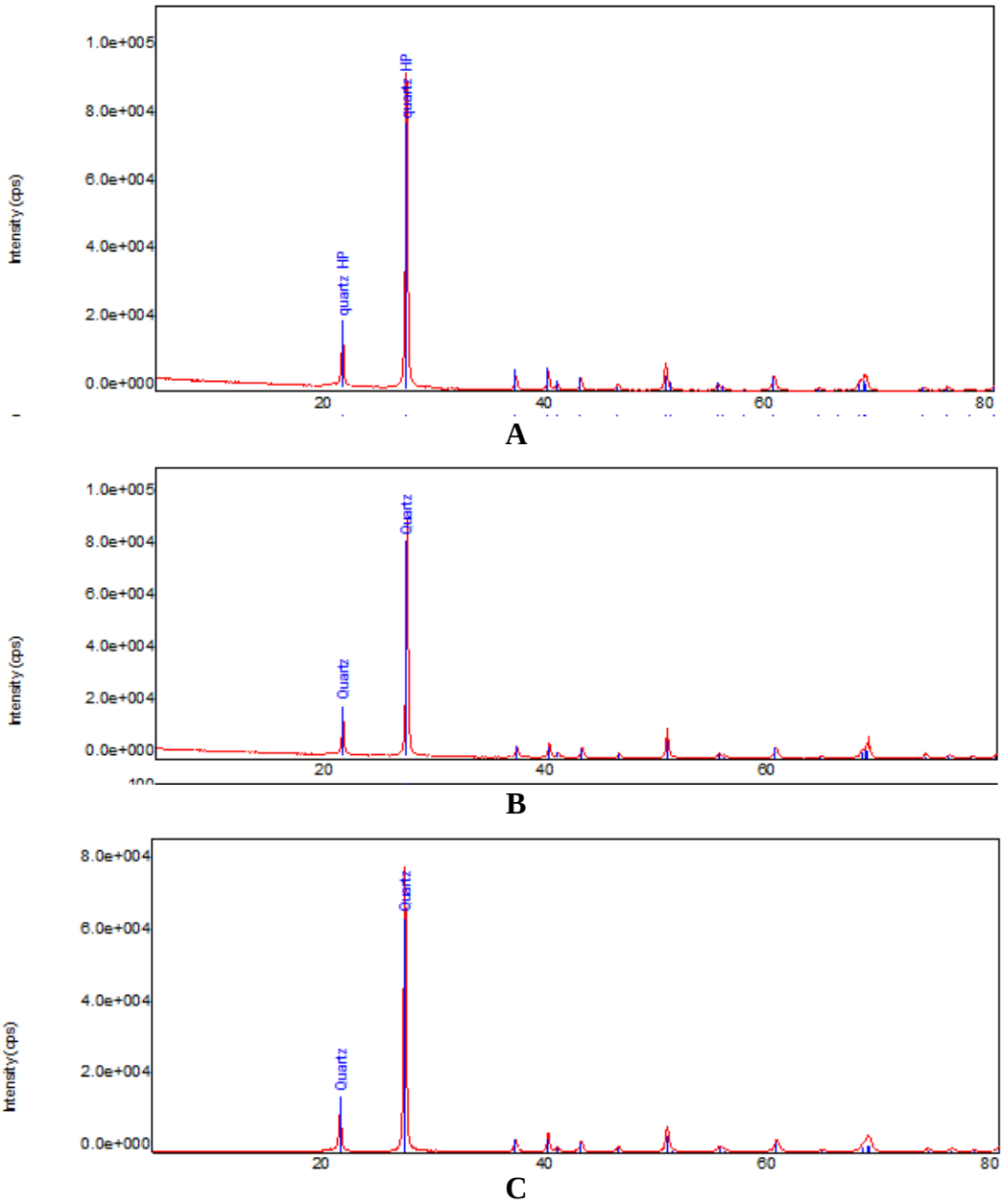

Figure 34. X-ray diffraction analyses show that quartz is the only silica phase present in all samples. **A)** XRD pattern of chert sample # 67: 100 % Quartz. **B)** XRD pattern of chert sample # 68: 100 % Quartz. **C)** XRD pattern of chert sample # 69: 100 % Quartz.

Table 3. Concentration of some trace elements in the carbonate samples in ppm.

Sample #	Na	Fe	K	Al
OAR-15-04	3.054	6.992	1.431	1.069
OAR-15-08	3.695	9.414	2.014	2.906
OAR-15-12	15.23	3.904	1.837	1.925
OAR-15-16	2.904	7.043	1.393	1.404
OAR-15-20	> 24.872	19.546	3.755	7.693
OAR-15-24	2.804	5.056	1.874	2.446
OAR-15-28	12.558	10.826	3.126	4.931
OAR-15-32	> 115.016	10.159	4.781	4.072
OAR-15-36	17.47	18.063	2.9	4.048
OAR-15-40	> 55.870	14.158	4.227	6.015
OAR-15-44	8.053	10.048	2.618	3.419
OAR-15-48	15.376	42.636	9.149	> 90.409
OAR-15-52	> 20.406	18.672	6.21	10.417
OAR-15-56	11.78	15.372	5.133	7.024
OAR-15-60	17.461	40.339	14.287	> 82.667

Table 4. Porosity and permeability results for selected carbonate samples.

Sample #	Porosity (%)	Permeability (mD)
OAR-15-01	6.561	0.0376
OAR-15-05	18.604	8.751
OAR-15-10	7.024	0.0778
OAR-15-11	5.256	0.0566
OAR-15-12	19.557	8.56
OAR-15-15	10.745	0.2029
OAR-15-18	7.709	0.0573
OAR-15-21	8.238	0.0365
OAR-15-26	11.668	0.3016
OAR-15-27	13.734	0.5916
OAR-15-31	9.171	0.1801
OAR-15-34	7.267	0.0244
OAR-15-35	11.252	0.1624
OAR-15-37	8.515	0.0549
OAR-15-38	10.169	0.0767
OAR-15-42	11.888	0.1378
OAR-15-47	11.918	0.217
OAR-15-52	10.302	0.0478
OAR-15-54	11.917	0.2986
OAR-15-55	10.458	0.0863
OAR-15-57	12.553	0.166
OAR-15-58	11.827	0.1629

CHAPTER 4 DISCUSSION

4.1 Chertification

Two mechanisms of chertification are recognized; replacement of carbonate by silica and replacement of evaporite nodules by silica. Cherts are replacing carbonate judging by the fabric-preserving texture of some cherts. Cherts are replacing evaporite precursor judging by relicts found within the cherts (Figure 29).

Hughes (2004 & 2009) considered that chert occurrences in the formation represents silica remobilization of concentrations of sponge spicules deposited during the maximum flooding of parasequences. In my study, the organic origin of silica was confirmed based on the abundance of sponge spicules in the chert (Figure 30-a) and the upper Tuwaiq Mountain carbonate (Figure 30-b).

4.2 Dedolomitization

4.2.1 Dedolomitization Distribution

The lowermost part is not affected by the calcitization process. This is supported by the increase in the dolomite concentration with depth and absence of calcite geodes. Thus, the lowermost part is considered a zone of no filtration of dedolomitizing fluid. On the other hand, the middle and upper parts are affected by the calcitization process. This is supported by the abundance of different textures of rhombohedral calcites and rhombohedral pores. Thus, the dedolomitizing fluid has infiltrated the upper and the middle

parts. The dedolomite microfabrics reflect the behavior and the characteristics of the dedolomitizing fluid (see next section).

4.2.2 Dedolomitization Microfabrics

Calcite does not commonly develop a rhombohedral habit in limestones. Therefore calcite partially or entirely filling rhomb-shaped pore space, or replacing dolomite crystals, constitutes the most straightforward evidence of dolomite calcitization (Coniglio, 1978). Various textures of rhombohedral calcites and rhombohedral pores have been recognized in the middle and upper part of the studied section.

Rhombohedral pores seem to be caused by dolomite dissolution or the selective leaching of mineralogically unstable high-magnesian calcite (Figure 35; Railsback, 1999), believed in many cases to be the initial product of dedolomitization (Evamy, 1967).

Drusy calcite cementation, which is dominant in the upper part, is observed to precipitate in the fractures and pore spaces (intergrains and dolomite molds). Porosity changes in two-step dolomite calcitization are expected depending on which step is dominant; dissolution or precipitation.

Pseudomorphic replacement, which is dominant in the middle part, was governed by the condition of equal volumetric rate for dolomite dissolution and calcite precipitation (one-step dolomite calcitization). No change in porosity is expected to take place where this mechanism of dolomite calcitization occurs. According to Longman (1980) “Meteoric waters have precipitated the excess calcium carbonate picked up in the vadose zone and reached equilibrium with the surrounding sediments by the time they get into the deeper

parts of the freshwater phreatic zone. Thus, little additional cementation occurs. Recrystallization may be an important process, but often occurs within the grains across a narrow front". In case of dedolomitization, the recrystallization occurs through a mechanism called 'coupled dissolution reprecipitation reactions' (CDR) causing the pseudomorphic replacement (Altree-Williams, 2015).

There are three main differences between calcite precipitated as cement and calcite precipitated as replacement during the dolomite calcitization process. First, calcite precipitated as cement occurs by two-step process (dissolution of dolomite then precipitation of calcite), while during calcite precipitated as replacement the dissolution and precipitation are closely spatially coupled at the interface between the dolomite and calcite. Second, calcite precipitated as cement does not necessarily preserve the external morphology of the parent dolomite (usually corroded), while calcite precipitated as replacement preserves the external morphology of the parent dolomite. Third, calcite precipitated as cement develops single or polycrystalline crystals without intracrystalline porosity and permeability, while calcite precipitated as replacement develops intracrystalline porosity and permeability which allows the fluid to maintain contact with the reaction front.

Numerous authors (e.g. Folk, 1974; Lahann, 1978) have commented on the diverse morphologies of calcite cements and have attempted to relate crystal morphology to the chemical environment of precipitation. Freshwater calcite cement crystals tend toward equant shapes, while marine calcite and aragonite cement crystals tend toward elongate fibrous shapes (Figure 36; Folk, 1974 redesigned by Moore & Wade, 2013). Based on the morphologies of the dedolomites, the solution causing the dedolomitization is meteoric.

The microfabrics of the dedolomites indicates different meteoric diagenetic environment (Figure 37; Longman, 1980 redesigned by Hartmann & Beaumont, 1999). The absence of the dedolomites in the lower part indicates that the meteoric solution responsible for the dolomite calcitization did not infiltrate this zone. This is supported by the increase of dolomite concentration and the absence of calcite geodes in the lower part. The middle part of the outcrop contains dedolomites characterized by pseudomorphic replacement texture. This type of texture is caused by meteoric water of stagnant nature (no circulation). This is supported by the similarity of the iron and sodium concentrations between the middle and lower parts. The cementation and solution textures displayed by the dedolomites in the upper part indicate phreatic active zone (causing different cementation textures) and late phreatic zone of solution or late vadose zone of solution (causing the rhombohedral pores texture). This is supported by wider range of porosities in the upper part and the lower concentration of iron and sodium caused by the circulated meteoric water.

4.2.3 Dedolomitization Mechanism

Dabbagh (2006) attributed the calcitization process to the dissolution of massive anhydrite deposits of the Arab and Hith Formations. An alternative explanation is given here based on the new finding of evaporate relicts within the chert nodules. The Jurassic formations consist predominantly of carbonates. Siliciclastics are interbedded within the Toarcian, Bajocian, and Bathonian Marrat and Dhruma formations. Evaporitic sediments become more common in the Kimmeridgian and Tithonian Arab and Hith formations. The lower part of the Tuwaiq Mountain Formation has been described in the literature to be

marly (Manivit et al., 1985; Vaslet et al., 1988; Vaslet et al., 1991). On the other hand, the existence of evaporites has never been reported in the Tuwaiq Mountain Formation.

Two lines of evidence reveal the presence of former evaporite nodules in the upper Tuwaiq Formation; carbonate pseudomorphs after lenticular gypsum (Figure 27) and presence of evaporite relicts within the chert nodules (Figure 29). Therefore, the vanished evaporite nodules are assumed to be the source of the Ca-rich solution necessary for the dolomite calcitization reaction.

4.2.4 Dedolomitization Timing

Partial dolomitization was widespread throughout the formation. The dolomitizing fluids were produced after evaporite precipitation. Then, chertification of organic origin replaced most of the evaporite and the surrounding carbonate. Later, meteoric water dissolved the remaining part of the evaporite causing dolomite calcitization to occur.

Figure 38 summarizes the findings and the interpretations of this study.

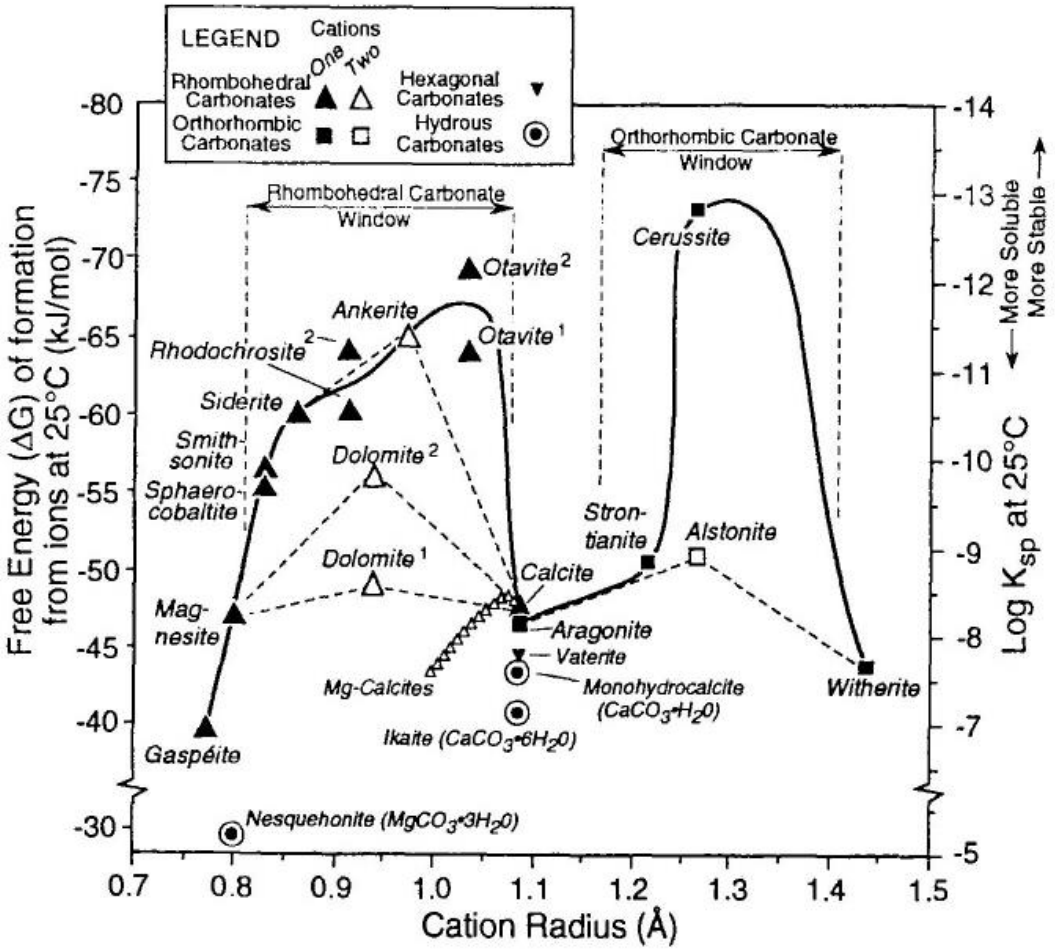

Figure 35. Plot of the free energy of formation from cations (left side) and solubility constants (right side) in rhombohedral carbonates (solid triangles) and orthorhombic carbonates (solid squares) with respect to cationic radius. Minerals higher in diagram are more stable (less soluble) (Railsback, 1999).

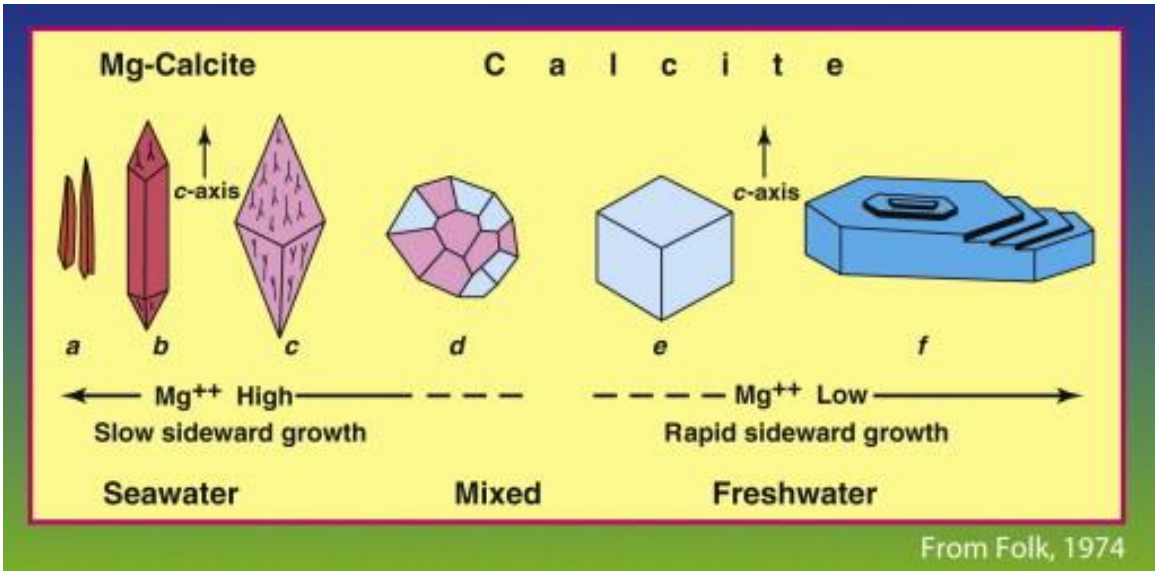

Figure 36. Calcite crystal growth habit as a function of Mg/Ca ratio (Folk, 1974 redesigned by Moore & Wade, 2013).

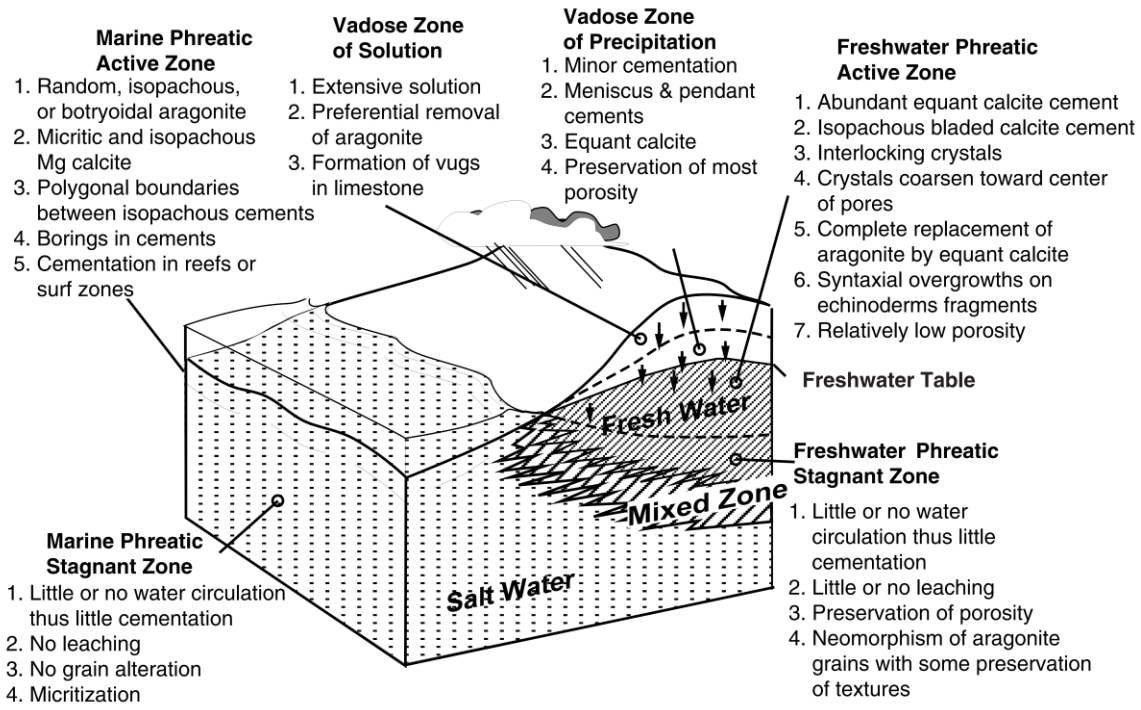

Figure 37. Block diagram summarizes early diagenetic processes and products that occur in carbonate environments (Longman, 1980 redesigned by Hartmann & Beaumont, 1999).

Table 5. Paragenetic sequence of events for Tuwaiq Formation carbonates in the study area. Both the terms 'early' and 'late' diagenesis should be conventionally understood as relative in time, rather than as indicating an absolute age.

Diagenetic sequence	**Early**	**Late**
Evapoirite precipitation		
Dolomitization		
Silicification		
Evaporite dissolution		
Dolomite calcitization		

My Findings								My Interpretation
Tuwaiq Zones	Field Observations		Chemistry		Porosity	Minerals	Petrography	Diagenetic Environment
	Chert	Calcite Geodes	Na	Fe	Ø		Dedolomite Texture & Distribution	
Upper	Y	Y	1	3	5-20%	Cal+Qz	Cementation and Dissolution Textures	Phreatic Active Zone and Late Phreatic Zone of Solution
	Y						Cementation Textures	Phreatic Active Zone
			4	5	10-12%		Cementation and Replacement Textures	Transitional Zone
Middle	N					Cal+Qz+Clay	Replacement Texture	Phreatic Stagnant Zone
Lower		N				Cal+Dol+Clay	No Dedolomitization	No filteration

Figure 38. Summary of the findings and their intepretation.

CHAPTER 5 CONCLUSIONS AND RECOMMENDATIONS

5.1 Conclusions

- Two diagenetic processes (chertification and calcitization) distinguish the Jurassic (late Callovian) upper Tuwaiq Mountain Formation (Daddiyah member).
- While chertification affected the Daddiyah member only, the dolomite calcitization process affects the Daddiyah member and part of the underlying member.
- Strong evidences (evaporite relicts and calcite pseudomorph after gypsum) confirm the former presence of evaporite within the upper Tuwaiq Formation.
- Cherts, of organic origin, are replacing a carbonate and evaporite precursor judging by the fabric-preserving texture and relicts found within the cherts.
- Vanished evaporite is suggested to be the driving force for the dolomite calcitization process. Dissolution of evaporite provides a calcium source necessary for the calcitization reaction to take place.
- Porosity changes appear to be related with the type of dedolomite texture. Replacement fabrics appear to have no effect on the porosity. The cementation fabric seems to decrease the porosity, while the dissolution fabrics increase it.
- The paragenetic sequence is interpreted as follows: 1) evaporite precipitation, 2) dolomitization, 3) chertification, 4) evaporite dissolution, 5) dolomite calcitization.

5.2 Recommendations

- Microsampling for cement would have given more indicative results about the diagenetic environment.
- Analysis of Insoluble residues should be performed on some samples that contain minute amounts of unidentified authigenic minerals.
- The $\delta^{18}O$ composition of the silica should be checked to confirm if the silica replacing carbonates is distinct from that replacing evaporite. The result of this will indicate if there are two separate sets of conditions for silicification or it is just one phase of replacement.

REFERENCES

Acero, P., F. Gutiérrez, J. P. Galve, L. F. Auqué, D. Carbonel, M. J. Gimeno, Javier B. Gómez, M. P. Asta, & Yechieli, Y. (2013). Hydrogeochemical characterization of an evaporite karst area affected by sinkholes (Ebro Valley, NE Spain). *Geologica Acta*, *11*(4), 389-407.

Al-Hashimi, W. S., & Hemingway, J. E. (1973). Recent Dedolomization and the Origin of the Rusty Crusts of Northumberland. *Journal of Sedimentary Research*, *43*(1), 82-91.

Al-Husseini, M. I. (1997). Jurassic sequence stratigraphy of the western and southern Arabian Gulf. *GeoArabia*, *2*(4), 361-382.

Altree-Williams, A., Pring, A., Ngothai, Y., & Brugger, J. (2015). Textural and compositional complexities resulting from coupled dissolution–reprecipitation reactions in geomaterials. *Earth-Science Reviews*, *150*, 628-651.

Arkell, W. J., Bramkamp, R. A., & Steineke, M. (1952). Jurassic Ammonites from Jebel Tuwaiq, Central Arabia. *Philosophical Transactions of the Royal Society of London. Series B, Biological Sciences*, *236*(633), 241–313.

Armenteros, I. (2010). Diagenesis of carbonates in continental settings. *Developments in Sedimentology*, *62*, 61-151.

Basyoni, M. H., & Khalil, M. (2013). An overview of the diagenesis of the Upper Jurassic carbonates of Jubaila and Hanifa formations, central Saudi Arabia. *Arabian Journal of Geosciences*, *6*(2), 557-572.

Bischoff, J. L., Juliá, R., Shanks, W. C., & Rosenbauer, R. J. (1994). Karstification without carbonic acid: Bedrock dissolution by gypsum-driven dedolomitization. *Geology*, *22*(11), 995-998.

Boni, M., Mondillo, N., & Balassone, G. (2011). Zincian dolomite: A peculiar dedolomitization case?. *Geology*, *39*(2), 183-186.

Boni, M., Mondillo, N., Balassone, G., Joachimski, M., & Colella, A. (2013). Zincian dolomite related to supergene alteration in the Iglesias mining district (SW Sardinia). *International Journal of Earth Sciences*, *102*(1), 61-71.

Braithwaite, C. J. R., & Heath, R. A. (2013). Alkali–carbonate reactions and "dedolomitization" in concrete: silica, the elephant in the corner. *Quarterly Journal of Engineering Geology and Hydrogeology*, *46*(3), 351–360.

Brasier, A. T., Fallick, A. E., Prave, A. R., Melezhik, V. A., Lepland, A., & Scientists, F. D. (2011). Coastal sabkha dolomites and calcitised sulphates preserving the Lomagundi-Jatuli carbon isotope signal. *Precambrian Research*, *189*(1), 193-211.

Braun, M., & Friedman, G. M. (1970). Dedolomitization Fabric in Peels: A Possible Clue to Unconformity Surfaces: NOTES. *Journal of Sedimentary Research*, *40*(1), 417-419.

Budai, J. M., Lohmann, K. C., & Owen, R. M. (1984). Burial dedolomite in the Mississippian Madison Limestone, Wyoming and Utah thrust belt. *Journal of Sedimentary Research*, *54*(1), 276-288.

Cantrell, D. L., Al-Khammash, A., & Jenden, P. D. (2007). Characterization and significance of dedolomite in Wadi Nisah, central Saudi Arabia. *GeoArabia*, *12*(3), 15-30.

Chilingar, G. V. (1956). Dedolomitization; a review. *AAPG Bulletin*, *40*(4), 762-764.

Coniglio, M. (1978). Dedolomitization. In *Sedimentology* (pp. 300-303). Springer Netherlands.

Dabbagh, M. E. (2006). Diagenesis of Jurassic Tuwaiq Mountain Limestone, central Saudi Arabia. *Journal of King Saud University*. *19*(1), 31-58.

De Groot, K. (1967). Experimental Dedolomitization. *Journal of Sedimentary Research*, *37*(4), 1216-1220.

Decrée, S., Marignac, C., De Putter, T., Deloule, E., Liégeois, J. P., & Demaiffe, D. (2008). Pb–Zn mineralization in a Miocene regional extensional context: the case of the Sidi Driss and the Douahria ore deposits (Nefza mining district, northern Tunisia). *Ore Geology reviews*, *34*(3), 285-303.

Dickson, J. A. D. (1966). Carbonate identification and genesis as revealed by staining. *Journal of Sedimentary Research*, *36*(2), 491-505.

El-Asa'ad, G. M. (1989). Callovian colonial from the Towaiq mountain limestone of Saudi Arabia. *Palaeontology*, *32*(3), 675-684.

El-Asa'Ad G.M.A. (1992). Late Callovian Ammonites from the Tuwaiq Mountain Limestone of Saudi Arabia. *Journal of King Saud University*, *4*(2), 173-184.

El-Hedeny, M., Hewaidy, A. and Al-Kahtany, Kh. (2012). Shallow-marine trace fossils from the Callovian-Oxfordian Tuwaiq Mountain Limestone and Hanifa

Formations, central Saudi Arabia. *Australian Journal of Basic and Applied Sciences, 6*(3), 722-733.

Eltom, H., Abdullatif, O., Makkawi, M., Al-Ramadan, K., & Abdulraziq, A. (2015). Porosity evolution within high-resolution sequence stratigraphy and diagenesis framework: outcrop analog of the upper Jurassic Arab-D reservoir, Central Saudi Arabia. *Arabian Journal of Geosciences, 8*(3), 1669-1690.

Enay, R., Mangold, C., Almeras, Y., & Hughes, G. W. A. G. (2009). The Wadi ad Dawasir" delta", central Saudi Arabia: A relative sea-level fall of Early Bathonian age. *GeoArabia*, *14*(1), 17-52.

Evamy, B. D. (1963). The application of a chemical staining technique to a study of dedolomitisation. *Sedimentology, 2*(2), 164-170.

Evamy, B. D. (1967). Dedolomitization and the Development of Rhombohedral Pores in Limestones. *Journal of Sedimentary Research, 37*(4). 1204-1215.

Fairbridge, R. W. (1978). Dedolomitization. *The Encylopedia of Sedimentology. Stroudsburg, Pennsylvania: Dowden, Hutchison and Ross Inc*, 233-235.

Flügel, E. (2004). Diagenesis, Porosity, and Dolomitization. In *Microfacies of Carbonate Rocks* (pp. 267-338). Springer Berlin Heidelberg.

Folk, R. L. (1974). The natural history of crystalline calcium carbonate; effect of magnesium content and salinity. *Journal of Sedimentary Research*, *44*(1), 40–53.

Friedman, G. M. (1965). Terminology of crystallization textures and fabrics in sedimentary rocks. *Journal of Sedimentary Research*, *35*(3), 643-655.

Friedman, G. M., & Sanders, J. E. (1967). Origin and occurrence of dolostones. *Developments in Sedimentology*, *9*, 267-348.

Gillott, J. E. (1964). Mechanism and kinetics of expansion in the alkali-carbonate rock reaction. *Canadian Journal of Earth Sciences*, *1*(2), 121-145.

Giménez-Montsant, J., Calvet, F., & Tucker, M. E. (1999). Silica diagenesis in Eocene shallow-water platform carbonates, southern Pyrenees. *Sedimentology*, *46*(6), 969-984.

Grainger, D. J. (2007). *The geologic evolution of Saudi Arabia: a voyage through space and time*. Jeddah: Saudi Geological Survey.

Hamidi, E. M., Colin, F., & Boulange, B. (1998). Mise en evidence d'un debut d'encroutement carbonate sur les basaltes du Trias dans le Moyen Atlas (Maroc). *Bulletin de la Societe Geologique de France*, *169*(1), 63-68.

Hanshaw, B. B., & Back, W. (1979). Major geochemical processes in the evolution of carbonate—Aquifer systems. *Journal of Hydrology*, *43*(1), 287-312.

Hartmann, D. J., & Beaumont, E. A. (1999). Predicting reservoir system quality and performance. *Exploring for oil and gas traps: AAPG Treatise of Petroleum Geology, Handbook of Petroleum Geology*, 9-1.

Hughes, G. (2008). Biofacies and palaeoenvironments of the Jurassic Shaqra group of Saudi Arabia. *Volumina Jurassica*, *6*, 33-45.

Hughes, G. W. (2004). Middle to Upper Jurassic Saudi Arabian carbonate petroleum reservoirs: Biostratigraphy, micropalaeontology and palaeoenvironments. *GeoArabia*, *9*(3), 79–114.

Hughes, G. W. (2009). Using Jurassic micropaleontology to determine Saudi Arabian carbonate paleoenvironments. *Geologic Problem Solving with Microfossils. SEPM, Special Publications*, *93*, 127-152.

Kargel, J. S., Schreiber, J. F., & Sonett, C. P. (1996). Mud cracks and dedolomitization in the Wittenoom Dolomite, Hamersley Group, Western Australia. *Global and Planetary Change*, *14*(1), 73-96.

Katz, A. (1968). Calcian Dolomites and Dedolomitization. *Nature*, *217*, 439–440.

Katz, A. (1971). Zoned Dolomite Crystals. *The Journal of Geology*, *79*(1), 38–51.

Khalifa, M. A. (2005). Lithofacies, diagenesis and cyclicity of the 'Lower Member'of the Khuff Formation (Late Permian), Al Qasim Province, Saudi Arabia. *Journal of Asian Earth Sciences*, *25*(5), 719-734.

Khalifa, M. A. (2012). Peritidal to intrashelf basin, facies transition of the Adgham Formation (Late Triassic) Al Qasim Province, Saudi Arabia. *Carbonates and Evaporites*, *27*(3-4), 299-319.

Lahann, R. W. (1978). A chemical model for calcite crystal growth and morphology control. *Journal of Sedimentary Research*, *48*(1), 337–347.

Lin, Y.S., Zhang, M.L., Qin, J.M., Jiang, G.H., Shu, L., Liu, Y., Yang, Y., Peng, W., Huang, X.Y., & Huang, F. (2009). On the transformation of Stalagmite texture and Structure. *Northwestern Geology*, *42*(3), 36–46.

Longman, M. W. (1980). Carbonate diagenetic textures from nearsurface diagenetic environments. *AAPG Bulletin*, *64*(4), 461-487.

Manivit, J., Pellaton, C., Vaslet, D., Le Nindre, Y. M., Brosse, J. M., Breton, J. P., & Fourniguet, J. (1985). Geologic map of the Darma quadrangle, sheet 24H, Kingdom of Saudi Arabia. *Saudi Arabian Deputy Ministry for Mineral Resources Geosciences Map, GM-101, scale*, *1*(250,000), 133.

Margolis, S. V. (1989). Authenticating ancient marble sculpture. *Scientific American*, *260*(6), 104-110.

Meyer, F. O., & Hughes, G. W. (2000). A multidisciplinary integration of selected Saudi Arabian carbonate unconformities: (abstract). *GeoArabia*, v. 5, p. 144.

Moore, C. H., & Wade, W. J. (2013). Carbonate Diagenesis: Introduction and Tools. *Developments in Sedimentology*, 67, 67–89.

Okla, S. M. (1987). Algal microfacies in Upper Tuwaiq mountain limestone (Upper Jurassic) near Riyadh, Saudi Arabia. *Palaeogeography, Palaeoclimatology, Palaeoecology*, *58*(1), 55-61.

Perkins, R. D. (1968). Primary Rhombic Calcite in Sedimentary Carbonates: NOTES. *Journal of Sedimentary Research*, *38*(4), 1371-1374.

Plummer, L. N., & Back, W. (1980). The mass balance approach: application to interpreting the chemical evolution of hydrologic systems. *American Journal of Science*, *280*(2), 130-142.

Powers, R. W. (1968). *Lexique Stratigraphique International: Saudi Arabia, Excluding Arabian Shield. Asie*. Centre National de la Recherche Scientifique.

Powers, R. W., Ramirez, L. F., Redmond, C. D., & Elberg Jr., E. L. (1966). *Geology of the Arabian Peninsula; sedimentary geology of Saudi Arabia* (USGS Numbered Series No. 560-D).

Prado-Pérez, A. J., & del Villar, L. P. (2011). Dedolomitization as an analogue process for assessing the long-term behaviour of a CO 2 deep geological storage: the Alicún de las Torres thermal system (Betic Cordillera, Spain). *Chemical Geology*, *289*(1), 98-113.

Purser, B. H. (1985). Dedolomite Porosity and Reservoir Properties of Middle Jurassic Carbonates in the Paris Basin, France. In P. O. Roehl & P. W. Choquette (Eds.), *Carbonate Petroleum Reservoirs* (pp. 341–355). Springer New York.

Rabier, C., Anguy, Y., Cabioch, G., & Genthon, P. (2008). Characterization of various stages of calcitization in Porites sp corals from uplifted reefs—Case studies from New Caledonia, Vanuatu, and Futuna (South-West Pacific). *Sedimentary Geology*, *211*(3), 73-86.

Railsback, L. B. (1999). Patterns in the compositions, properties, and geochemistry of carbonate minerals. *Carbonates and Evaporites*, *14*(1), 1-20.

Raines, M. A., & Dewers, T. A. (1997). Dedolomitization as a driving mechanism for karst generation in Permian Blaine Formation, Southwestern Oklahoma, USA. *Carbonates and Evaporites*, *12*(1), 24–31.

Rausch, R., Simon, T., Al Ajmi, H., & Dirks, H. (2014). The scarp lands of Saudi Arabia. *Arabian Journal of Geosciences*, *7*(6), 2437-2450.

Rogala, B., James, N. P., & Calver, C. R. (2010). Diagenesis of early Permian high-latitude limestones, Lower Parmeener Supergroup, Tasmania. *Sedimentology*, *57*(7), 1771-1790.

Scholle, P. A., & Ulmer-Scholle, D. S. (2003). *A Color Guide to the Petrography of Carbonate Rocks: Grains, Textures, Porosity, Diagenesis, AAPG Memoir 77* (Vol. 77). AAPG.

Shearman, D. J., Khouri, J., & Taha, S. (1961). On the replacement of dolomite by calcite in some mesozoic limestones from the French Jura. *Proceedings of the Geologists' Association*, *72*(1), 1–IN3.

Smit, D. E., & Swett, K. (1969). Devaluation of 'dedolomitization'. *Journal of Sedimentary Research*, *39*(1), 379-380.

Stafford, K. W., Ulmer-Scholle, D., & Rosales-Lagarde, L. (2008). Hypogene calcitization: Evaporite diagenesis in the western Delaware Basin. *Carbonates and Evaporites*, *23*(2), 89-103.

Taj, R. J. (2013). Microfacies, diagenesis, and depositional environments of the Tertiary carbonates of Usfan Formation in Haddat Ash Sham area, Western Arabian Shield, Saudi Arabia. *Arabian Journal of Geosciences*, *6*(4), 1011-1031.

Vaslet, D., Al-Muallem, M. S., Maddeh, S. S., Brosse, J. M., Fourniquet, J., Breton, J. P., & Le Nindre, Y. M. (1991). Explanatory notes to the geologic map of the Ar Riyad Quadrangle, Sheet 24 I, Kingdom of Saudi Arabia. Saudi Arabian Deputy Ministry for Mineral Resources, Jeddah. *Geosciences Map*, *121*, 1-54.

Vaslet, D., Brosse, J. M., Breton, J. P., Manivit, J., Le Strat, P., Fourniguet, J., & Shorbaji, H. (1988). Geologic map of the Shaqra quadrangle, sheet 25 H.*Kingdom of Saudi Arabia: Deputy Ministry for Mineral Resources Geoscience Map GM-120C*, *29*.

Vaslet, D., Manivit, J., Le Nidre, Y. M., Brosse, J. M., Fourniguet, J., & Delfour, J. (1983). Explanatory notes to the geologic map of the Wadi Ar Rayn Quadrangle. *Deputy Ministry for Mineral Resources, Jeddah*.

Von Morlot, A. (1847). Ueber Dolomit und seine künstliche Darstellung aus Kalkstein. *Naturwissenschaftliche Abhandlungen Gesammelt, und durch Subscription Hrsg, von Wilhelm Haidinger*, 1, 305–315.

Youssef, M., & El-Sorogy, A. S. (2015). Paleoecology of benthic foraminifera in coral reefs recorded in the Jurassic Tuwaiq Mountain Formation of the Khashm Al-Qaddiyah area, Central Saudi Arabia. *Journal of Earth Science*, *26*(2), 224-235.

Vitae

Name	:Omar Atef Radwan
Nationality	:Egyptian
Date of Birth	:9/22/1989
Email	:o.a.radwan@gmail.com
Address	:10 Alshaikh Zayed St, Zagazig, Egypt
Academic Background	:BSc in Geology and Chemistry, Zagazig University, Egypt
Research Interest	:Mineral characterization techniques; industrial minerals; sedimentary petrology
Publications	1. (Prepared to be submitted) Chertification and calcitization in the upper Tuwaiq Mountain Formation, Riyadh, Saudi Arabia. Co-authors: Ahmet U. Dogan, Michael A. Kaminski, Mohamed A. Morsy, Eric Christiansen. 2. (Prepared to be submitted) Dolomite calcitization (Dedolomitization) in Carbonate Sedimentology. Co-author: Dave Cantrell